Archives of Computational Methods in Engineering
https://doi.org/10.1007/s11831-026-10516-8

REVIEW

Coupled Chemo-Mechanical Simulation of Geosynthetic-Reinforced Subgrades: A Critical Review of Computational Models and Predictive Methods

Nur Rasfina Mahyan[1,2] · Mastura Azmi[1] · Fauziah Ahmad[1] · Siti Noor Linda Taib[3]

Received: 5 August 2025 / Revised: 12 January 2026 / Accepted: 14 February 2026

Abstract

The durability and resilience of geosynthetic-reinforced subgrades are increasingly threatened by coupled environmental and mechanical stressors, particularly in infrastructure systems exposed to cyclic traffic loads and chemically aggressive conditions such as acid rain, landfill leachates, and saline intrusion. This review provides a critical and systematic synthesis of current research on the chemo-mechanical behavior of reinforced subgrades, with an emphasis on the computational modeling approaches used to simulate their long-term performance. Particular attention is given to finite element models, damage mechanics frameworks, and multi-physics coupling techniques that capture the synergistic deterioration mechanisms arising from chemical degradation and repeated loading. The analysis compares behavior in homogeneous and layered soil systems, emphasizing the complexities of interface interactions, load transfer mechanisms, and degradation pathways of geosynthetics in soil. Current experimental protocols for chemical aging and mechanical testing are reviewed to assess their role in calibrating and validating numerical models. Despite growing interest in coupled modeling, significant gaps remain in integrating chemical transport, time-dependent material degradation, and dynamic loading into unified predictive frameworks. This paper further explores the potential of machine learning-assisted surrogate models, multi-scale simulations, and lifecycle-based computational strategies to support the design of resilient infrastructure. By bridging experimental insights with advanced numerical tools, this review advances the development of sustainable and adaptive ground reinforcement systems, aligning with the objectives of computational engineering and global infrastructure resilience goals.

1 Introduction

The integrity and longevity of infrastructure systems, particularly unpaved roads and low-volume pavements are significantly influenced by the mechanical performance of subgrades. In recent years, geosynthetic reinforcements, including geotextiles, geogrids, and geocomposites, have been widely used to enhance subgrade stiffness, minimize permanent deformation, and improve load distribution [1, 2]. While traditional reinforcement studies have primarily focused on static performance enhancement, there is a growing recognition that long-term durability is increasingly challenged by multi-axial environmental stressors, particularly in tropical and urbanized regions. Subgrades reinforced with geosynthetics are frequently exposed to cyclic mechanical loads from traffic and chemical attacks from environmental contaminants, including acid rain, landfill leachates, and saline groundwater [3, 4]. These coupled chemo-mechanical interactions progressively deteriorate the properties of both soils and geosynthetics, leading to microstructural damage, weakening of the interface, and eventual loss of load-bearing capacity [5, 6]. Since the rates of reaction kinetics, transport, and creep of these processes are temperature-dependent, we interpret degradation in a thermo-chemo-mechanical perspective while retaining a chemo-mechanical focus [7–9]. Unlike prior reviews that

✉ Mastura Azmi
cemastura@usm.my

1 School of Civil Engineering, Universiti Sains Malaysia, Nibong Tebal 14300, Malaysia

2 Centre for Pre-University Studies, Universiti Malaysia Sarawak, Kota Samarahan 94300, Malaysia

3 Department of Civil Engineering, Universiti Malaysia Sarawak, Kota Samarahan 94300, Malaysia

Published online: 27 February 2026

treat durability or mechanics in isolation, this article centers on fully coupled computational formulations and their synthesis with data-driven surrogates and digital-twin workflows, translating laboratory chemo-mechanical evidence into deployable prediction tools.

This article highlights four specific advances over previous reviews: (i) it formalizes implementation-level coupling patterns, including operator-splitting with User Material (UMAT), User Define Field (USDFLD), and User Element (UEL) state updates for chemo-mechanical degradation, explicitly treating temperature as a rate moderator (Arrhenius/Williams-Landel-Ferry (WLF)) rather than as a new governing field; (ii) it formalizes a chemistry-sensitive interface law and a two-step calibration process (constant-chemistry soaking + cyclic shear/plate loading) that directly integrates into finite element models (FEM) and continuum damage mechanics (CDM); (iii) it distinguishes homogeneous versus layered subgrade responses and links them to interface processes (shear localization, abrasion, bond softening) that control settlement; and (iv) it proposes a standardized benchmarking framework, including exposure matrices, interface-law identification, 3D/field validation, and uncertainty quantification, by integrating machine learning (ML)-FEM surrogates and digital-twin pipelines to make models ready for lifecycle management.

The practical need for this integration becomes evident when considering the measurable economic penalties associated with subgrade-driven pavement deterioration costs. The stakes are material, as pavement roughness directly raises road-user costs. Each 1 m/km rise in international roughness index (IRI) increases passenger-car fuel consumption by about 2–3% (and 1–3% for heavy trucks, depending on speed), thereby elevating network-wide vehicle operating costs when deterioration is left unchecked [10]. On the agency side, preventive preservation strategies reduce costs by approximately 25% per lane-mile compared with rehabilitation-only policies, based on statewide benchmarking of implemented programs [11]. Project-level studies echo these savings; for example, full-lane micromilling to restore surface quality yielded approximately $60,000 per lane-mile in direct cost savings while improving ride and extending service life [12]. These quantitative burdens and savings reinforce the need for durability-aware, coupled chemo-mechanical modeling and lifecycle decision tools.

Figure 1 illustrates the thermo-chemo-mechanical degradation sequence: cyclic loading drives fatigue crack initiation and growth, while chemical ingress alters microstructure and weakens the soil-geosynthetic bond. Superimposed temperature fields involving diurnal/seasonal cycles, as well as localized reaction-heat zones, accelerate the hydrolysis/oxidation kinetics (Arrhenius-type) and enhance viscoelastic creep/relaxation, thereby hastening interface softening and stiffness loss. The combined action of load, chemistry, and temperature therefore amplifies the reduction in strength and deformation in the reinforced system [13, 14]. Additionally, the degradation response varies significantly between homogeneous and layered soil systems, primarily due to differences in stress redistribution, thermal damping, moisture retention, and chemical permeability. As such, computational modeling must not only capture the independent effects of chemical and mechanical stressors but also the synergistic interactions at soil-geosynthetic interfaces under realistic boundary conditions. Despite advances in material characterization and soil-structure interaction models, most current engineering practices continue to rely on empirical and semi-empirical design frameworks. As demonstrated in Fig. 2, the evolution of subgrade modeling has progressed from basic California Bearing Ratio (CBR) correlations and Mohr-Coulomb formulations to more sophisticated multi-physics chemo-mechanical simulations (with temperature modulation) and, more recently, Artificial Intelligence (AI)-assisted predictive analytics. However, fully integrated chemo-mechanical simulations remain limited, and there is a pressing need for validated computational tools that can simulate time-dependent degradation under field-relevant stress and temperature conditions.

Furthermore, chemical degradation is not a monolithic process. As outlined in Table 1, various environmental stressors ranging from acidic leachates to saline or alkaline exposure impact geosynthetics through distinct pathways, including hydrolysis, plasticization, or stress corrosion cracking. These mechanisms are influenced by the type of geosynthetic polymer, soil chemistry, temperature history, and the duration of exposure, underscoring the complexity of developing robust degradation models for predicting long-term performance [8, 23, 24]. Despite this knowledge, most degradation models remain uncoupled, addressing either chemical or mechanical factors in isolation. This significantly limits their predictive capacity in real-world applications, where multi-physics interactions dominate. There is a critical need for computational frameworks that can simultaneously capture chemical transport, temperature-dependent reaction kinetics, creep, material aging, interface weakening, and mechanical fatigue, particularly when used in lifecycle performance simulations of reinforced soil systems.

To benchmark current capabilities and identify the remaining gaps, we next conducted a structured review of the literature. We conducted a structured literature scan (Scopus and Web of Science, 2000–2025; English) using combined keywords for temperature/thermal effects, geosynthetics, interface, diffusion/transport, hydrolysis/oxidation, FEM/CDM, multiphysics, surrogate/ML, and digital twin. Records were screened for (i) explicit chemo-mechanical

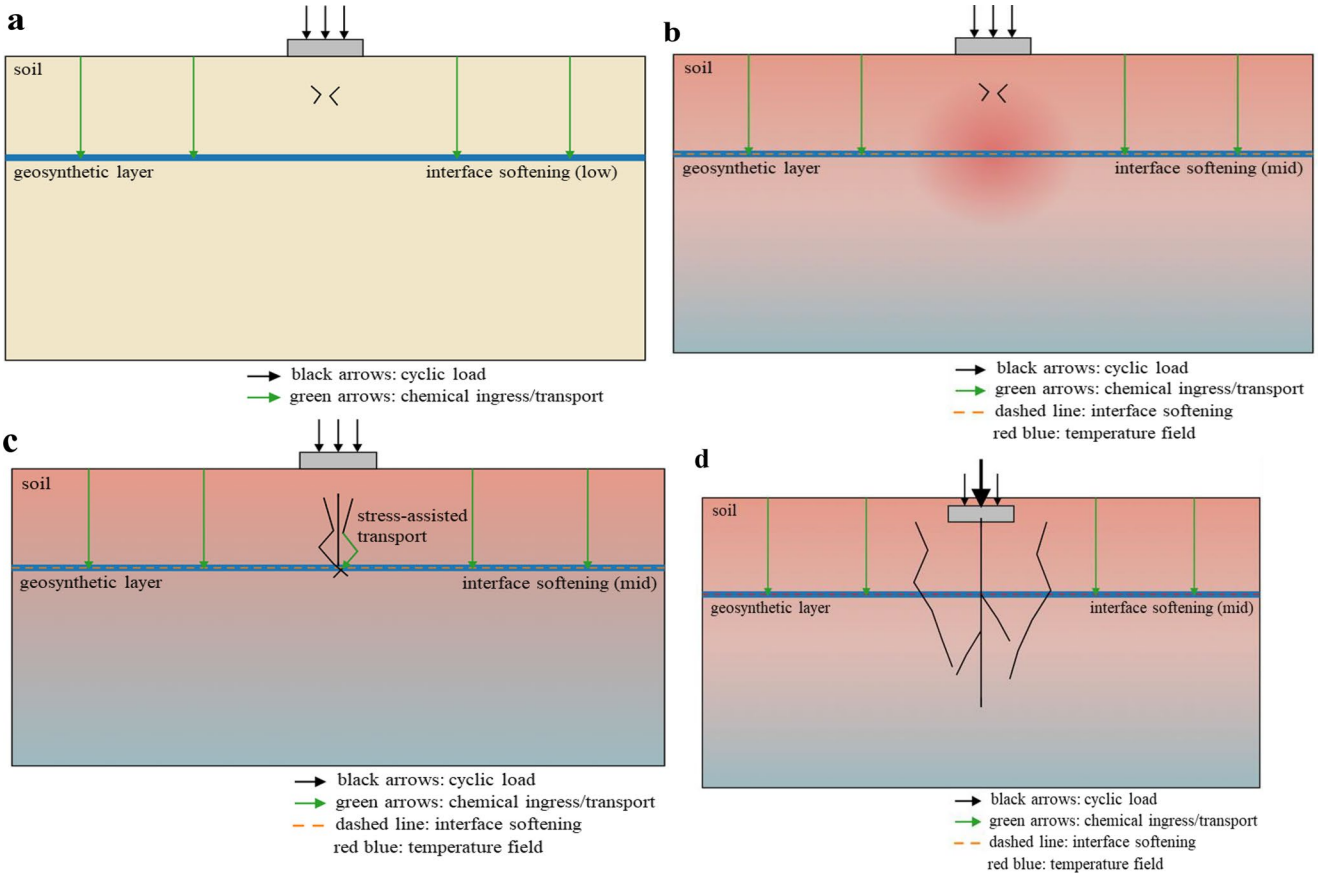

Fig. 1 Thermo-chemo-mechanical degradation sequence in geosynthetic-reinforced subgrades: **a** Initiation under cyclic loading with early chemical ingress, **b** Temperature influence (ambient cycles/reaction heat), accelerating hydrolysis/oxidation and viscoelastic creep **c** Stable crack growth with stress-assisted transport and temperature-dependent interface softening, and **d** crack coalescence, stiffness collapse, and loss of bearing capacity

content with temperature modulation where available, (ii) computational implementation details (constitutive law, coupling, or solver), and (iii) calibration/validation against lab or field data. Reference lists of eligible items were snowballed; standards/handbooks were included only when informing modeling choices.

This review aims to critically evaluate and synthesize the current state of computational modeling in the coupled chemo-mechanical analysis of geosynthetic-reinforced subgrades, explicitly noting the thermal influences that affect kinetics or creep. The paper emphasizes multi-physics simulation strategies, such as FEM, CDM, transport-reaction coupling, and data-driven surrogate tools. The specific objectives are to systematically review existing numerical models that simulate coupled chemical and mechanical deterioration in reinforced soils; examine how thermal–chemical aging and mechanical test data are used for model calibration and validation; assess the implementation of damage evolution laws, interface degradation models, and multi-scale frameworks; and explore the growing significance of machine learning, digital twins, and lifecycle analytics in supporting the design of adaptive infrastructure. This review contributes a novel perspective by bridging computational geomechanics, polymer durability science, and artificial intelligence, ultimately facilitating the development of resilient, adaptive, and sustainable ground reinforcement systems.

2 Problem Context and Engineering Challenges

2.1 Degradation Mechanisms in Geosynthetic-Reinforced Subgrades

Geosynthetics used in reinforced subgrades are subject to various degradation factors in the field, particularly in tropical and semi-urban areas, where they encounter acid rain, saline groundwater, landfill leachate intrusion, seasonal/diurnal temperature cycles, and cyclic vehicular load stress. These stimuli induce degradation via three key pathways: chemical, mechanical, and most critically,

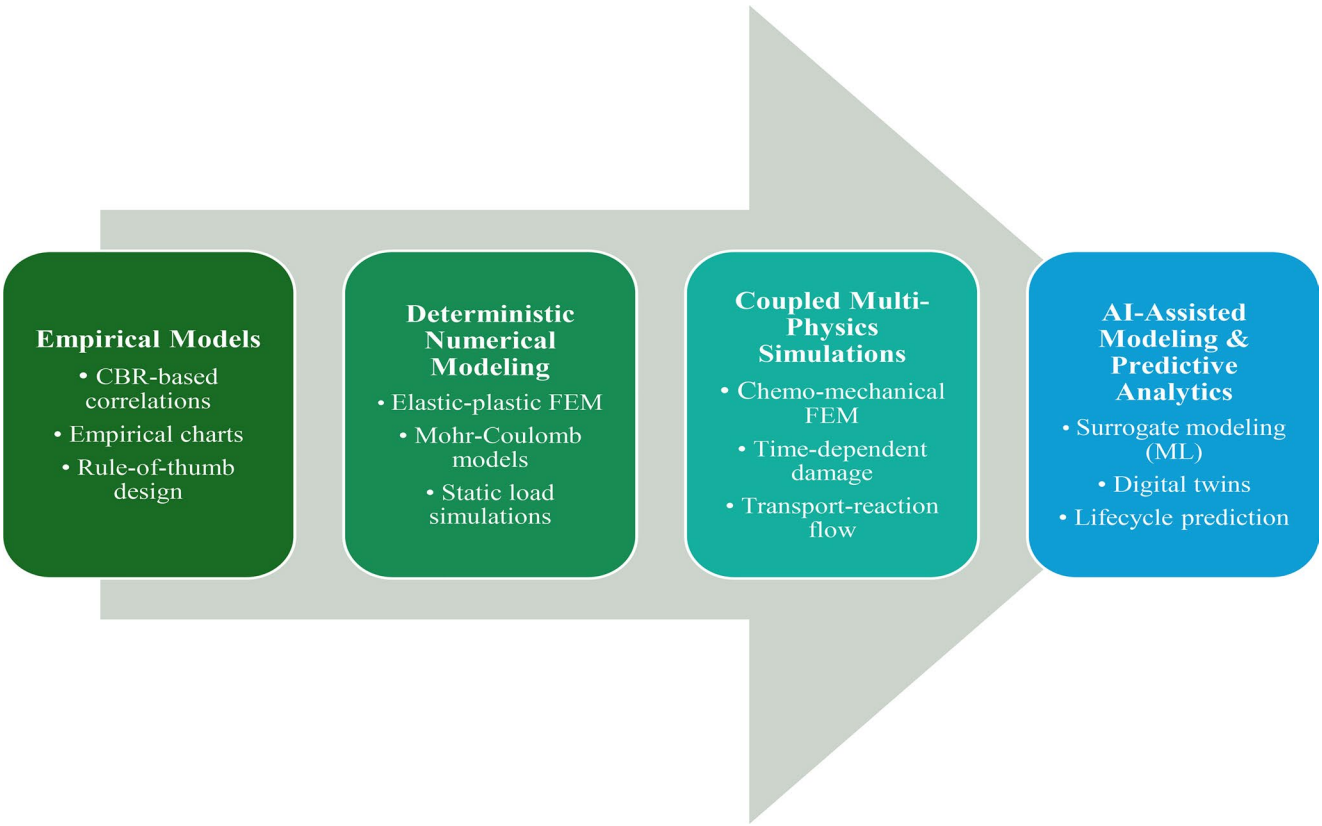

Fig. 2 Role of computational modeling in subgrade design

Table 1 Comparative summary of environmental stressors and their effects on geosynthetics

Environmental Stressor	Chemical Agent(s)	Affected Geosynthetic Types	Primary Degradation Mechanism	Typical Performance Impacts	Reference
Acidic Leachates	Sulfuric acid (H_2SO_4), Nitric acid (HNO_3), Organic acids	Polyester (PET), Polyamide (PA), Polypropylene (PP)	Hydrolysis of ester linkages in PET; chain scission in PA	Reduction in tensile strength, molecular weight loss, fiber embrittlement	[9, 15]
Sulfate Attack	Magnesium sulfate ($MgSO_4$), Sodium sulfate (Na_2SO_4)	PET, High Density Polyethylene (HDPE), Polyolefins	Stress corrosion cracking, crystallinity changes	Loss of elongation at break, stiffness reduction	[16, 17]
Saline/Chloride Contamination	Sodium chloride (NaCl), Calcium chloride ($CaCl_2$)	HDPE, PP, PET	Osmotic imbalance, polymer softening, chemical diffusion	Increased permeability, polymer swelling, loss of durability	[18, 19]
Alkaline Conditions	Calcium hydroxide ($Ca(OH)_2$), Sodium hydroxide (NaOH)	PET, PA	Alkali hydrolysis, surface erosion	Loss of ductility, stress cracking	[20]
Organic Contaminants	Hydrocarbons, landfill leachates	HDPE, PP	Plasticization, oxidative degradation	Polymer softening, time-dependent creep deformation	[21, 22]

chemo-mechanical coupling, with thermal conditions acting as a rate modulator. While each pathway can independently impair geosynthetic performance, their interaction often leads to accelerated and nonlinear deterioration. Chemical degradation mechanisms vary depending on the type of geosynthetic polymer and exposure conditions. For instance, PET undergoes ester hydrolysis under acidic conditions ($pH < 5$), resulting in chain scission and a loss of tensile strength [25]. Conversely, HDPE and PP are more susceptible to oxidative degradation, especially in the presence of saline and sulphate-rich environments, as indicated by [7, 26]. Table 2 consolidates representative findings from recent studies, demonstrating how exposure to different chemical agents, including sulfuric acid, chlorides, sulfates, and landfill leachates, leads to specific degradation modes such as plasticization, surface embrittlement, and ion-induced softening.

Table 2 Summary of synergistic chemo-mechanical effects reported in recent experimental studies

Geosynthetic Type	Chemical Agent	Loading Type	Observed Interaction	Reference
PET	Sulfuric acid (pH 3–4)	Uniaxial static and cyclic	Tensile strength and elongation were reduced more significantly under combined acid and load conditions.	[27]
PET Geogrid	Acidic leachate	Cyclic plate load	The bond strength at the soil-geogrid interface decreased by 35%, accompanied by a degradation in stiffness.	[28]
HDPE Geomembrane	Saline solution (NaCl, $CaCl_2$)	No mechanical loading	Oxidative degradation and permeability changes require coupling with mechanical data.	[29]
Woven PET Geotextile	Organic acid + sulfate	Cyclic triaxial	Stiffness loss accelerated with increasing soaking time under cyclic load.	[30]
PET Geotextile	Acidic rain simulator	Repeated load plate test	Creep deformation increased by 42% in chemically exposed samples compared to the control.	[31]

Building on these chemical pathways, thermal conditions act as modulators, accelerating or retarding reaction kinetics and creep without introducing a new mechanism. Reaction enthalpy, whether exothermic (heat-releasing) or endothermic (heat-absorbing), along with ambient temperature changes, influences both chemical kinetics and viscoelastic creep; thermally accelerated oxidation/hydrolysis of polymers is well documented [32]. In practice, the pore-fluid chemistry and polymer degradation rates accelerate with temperature (Arrhenius-type sensitivity), as shown for PET hydrolysis and HDPE geomembrane ageing in long-term studies [33]. Creep/relaxation in geosynthetics follows time–temperature superposition (TTS) using WLF/Arrhenius shift factors. For buried subgrades, diurnal fluctuations are largely attenuated and phase-lagged with depth by the pavement and base layers; thus, temperature typically acts as a moderator of the dominant chemistry and load mechanisms rather than a primary driver. We therefore treat temperature explicitly but parsimoniously in the modeling that follows.

We next consider how cyclic loading interacts with these thermally modulated chemical processes to drive fatigue and interface degradation. Under repeated vehicle loading, reinforced subgrades undergo fatigue-driven mechanical degradation, characterized by creep deformation, microcrack initiation, and interface slippage. The nature of stress transfer between the soil and the geosynthetic plays a crucial role in this process. Cyclic plate loading on PET geogrid-reinforced soil has been reported to reduce interface bond strength by 35% in acidic leachate environments [28]. Similarly, a 42% increase in creep deformation under repeated loading was observed after acid-rain conditioning in PET-reinforced specimens [31], highlighting that loading severity exacerbates degradation in chemically exposed samples. Rather than acting independently, chemical and mechanical degradation interact synergistically, producing compound effects that cannot be captured by linear superposition. As conceptualized in Fig. 1, cyclic loading facilitates crack propagation, increasing pore connectivity and allowing deeper chemical infiltration. In contrast, chemical attack simultaneously weakens polymer bonds and reduces ductility, amplifying susceptibility to fatigue failure. Table 2 summarizes these effects across different experimental studies, emphasizing that such degradation is both material-dependent and loading-specific.

2.2 Influence of Soil Configuration

The behavior and degradation of geosynthetics are highly sensitive to the configuration of the soil profile, specifically whether it is homogeneous or layered, with seasonal/diurnal temperature cycles largely attenuated with depth but still modulating reaction rates and creep. In homogeneous systems (e.g., lateritic clay), stress and chemical infiltration are distributed uniformly throughout the system. Figure 3(a) illustrates that vertical loading primarily leads to compressive fatigue and deep chemical ingress due to the uninterrupted pore network. This setup causes even modulus decline, which, although slow, shows no early warning signs and can lead to extensive subgrade instability. Layered subgrades, especially common in tropical road construction (e.g., sand over lateritic clay), present far more complex degradation pathways. As illustrated in Fig. 3(b), geosynthetics positioned at the interface of two soil layers experience horizontal shear, mechanical abrasion, and differential chemical attack due to disparate permeability and stiffness properties of the layers. Since the two soil layers differ in stiffness and permeability, shear and abrasion localize at the geosynthetic plane. These localization bands become preferential paths for chemical ingress and debonding; even modest thermal modulation at depth can accelerate local reaction kinetics and creep, allowing failure to nucleate while the surrounding soil appears intact. Figure 4 further conceptualizes this progression by mapping out five sequential stages: from initial chemical exposure and cyclic loading (Step 1) to interface softening (Step 2), crack formation (Step 3), stiffness degradation (Step 4), and eventually loss of load capacity and functional instability (Step 5). This structured flow provides a process-based lens through

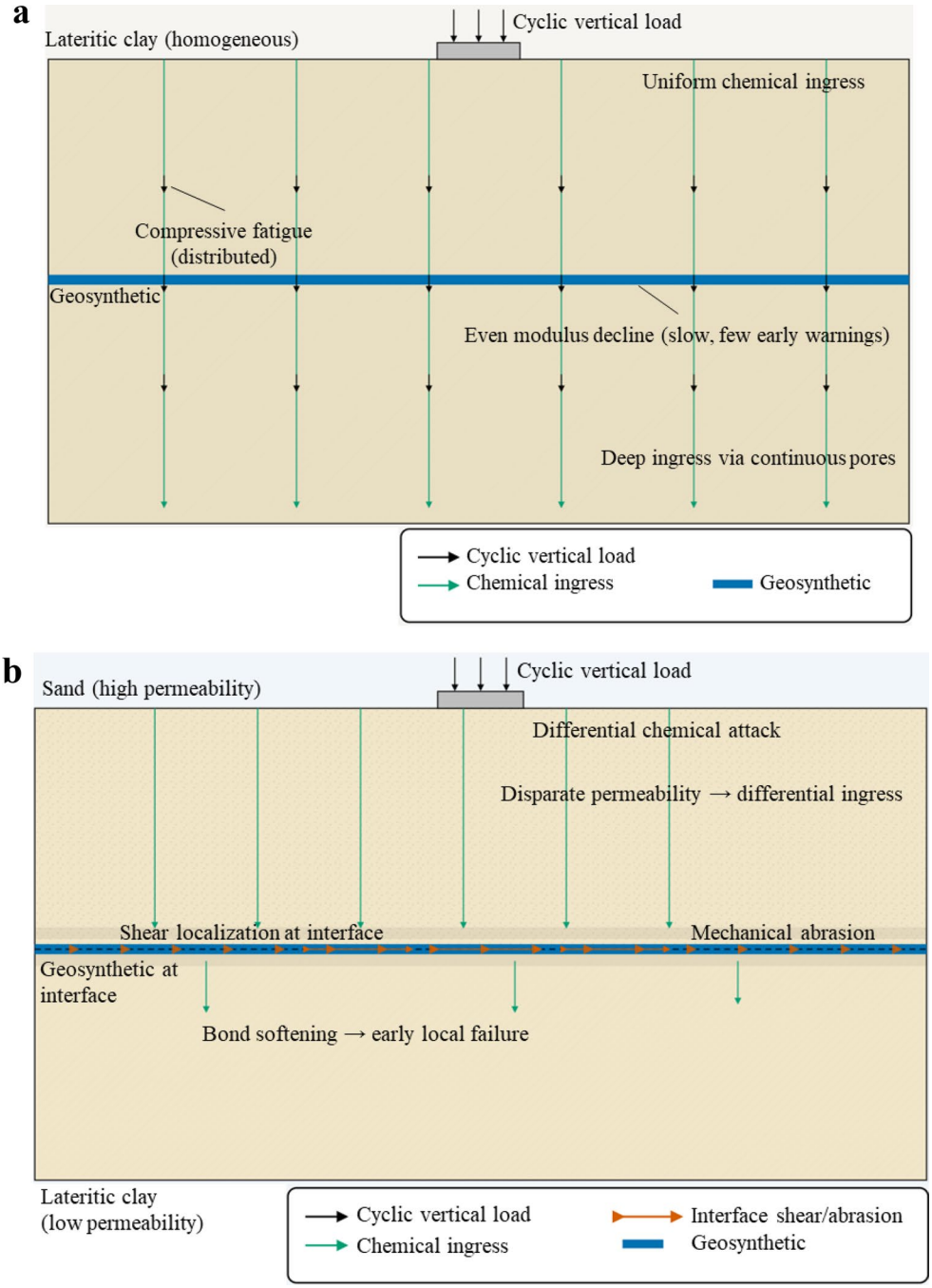

Fig. 3 **a** Homogeneous subgrade with embedded geosynthetic, **b** Layered subgrade with geosynthetic at the interface

which the mechanics of failure in layered systems can be predicted and modeled.

2.3 Motivation for Coupled Simulation Frameworks

Traditional simulation frameworks in geotechnical engineering are inadequate to capture the multi-physics, time-dependent nature of degradation in geosynthetic-reinforced systems. Linear elastic-plastic models (e.g., Mohr-Coulomb) do not account for chemical reaction kinetics, diffusion transport, or stiffness evolution under fatigue [34–36]. As degradation advances, the geosynthetic's tensile modulus, interface shear strength, and pore connectivity are no longer constants, but variables influenced by chemical concentration, depth-filtered temperature, and cyclic stress intensity. Hence, there is an urgent need to transition toward multiphysics chemo-mechanical (with thermal modulation) modeling frameworks capable of simulating transport–reaction–mechanical feedback, where chemical diffusion alters material properties and vice versa. Interface degradation dynamics, where the interaction between soil and geosynthetic materials deteriorates based on the stress history and

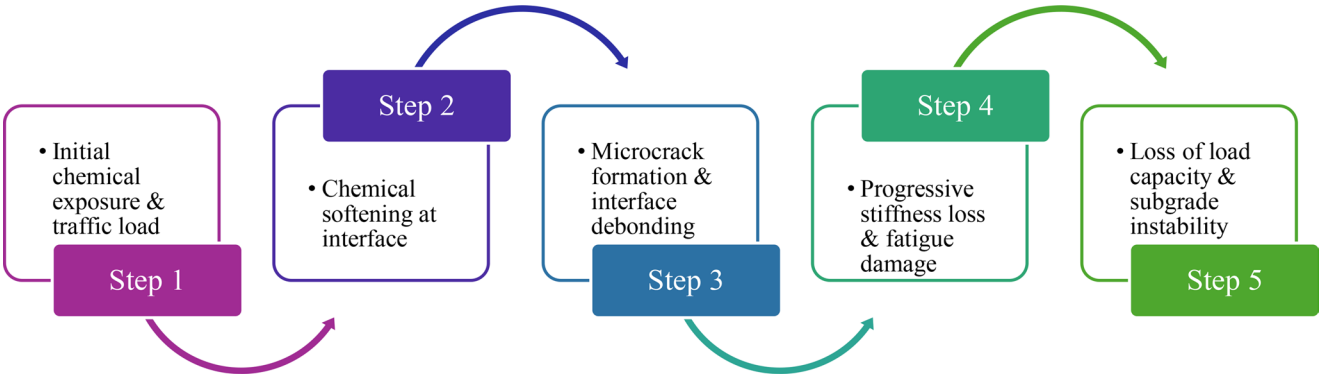

Fig. 4 Flow of degradation progression in layered subgrade under combined chemical and mechanical stress

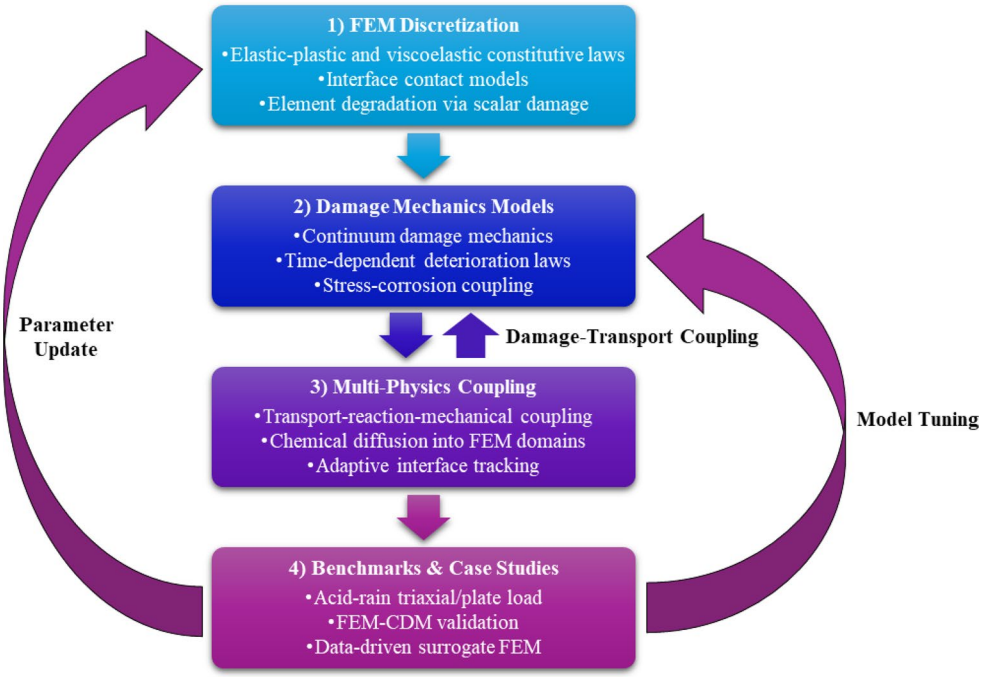

Fig. 5 Process flow and calibration logic for coupled chemo-mechanical modeling

exposure. Time-dependent property evolution, incorporating data from aging and triaxial fatigue testing for model calibration. Emerging works by [37, 38] have introduced finite element formulations that embed chemical damage laws within mechanical stress-strain relations. These studies highlight the potential of surrogate machine learning models and multi-scale damage algorithms to enhance computational efficiency, thereby facilitating the integration of these models into lifecycle-based infrastructure design.

3 Review of Computational Methods for Coupled Chemo-Mechanical Simulation

The modeling of chemo-mechanical degradation in geosynthetic-reinforced subgrades requires a multi-layered computational framework capable of simulating time-dependent, nonlinear interactions across soil-reinforcement interfaces, with temperature treated as a rate modulator. This section systematically reviews current modeling approaches, including FEM, CDM, and multi-physics coupling strategies, followed by an appraisal of benchmark studies and case applications. Figure 5 serves as a unifying visual narrative for this section, illustrating the methodological continuum from empirical FEM formulations to advanced coupled transport–mechanics (with optional temperature modulation) simulations and data-driven validations. The progressive layering from simple elasticity to full transport-reaction coupling mirrors the increasing demand for accuracy, scalability, and sustainability in subgrade design. Figure 5 summarizes the modeling pathway from constitutive choice (FEM), through damage evolution (CDM), to coupled transport–mechanics closed by benchmarking loops that update parameters and tune models. To guide model selection and

benchmarking in coupled analyses, Table 3 compares FEM, CDM, and Multiphysics frameworks, summarizing their core strengths, typical limitations, computational costs, coupling maturity, best-fit use cases, and representative exemplars.

3.1 Finite Element Modeling

Finite element methods are the basis of geotechnical simulation, offering flexibility in handling complex boundary conditions and heterogeneous materials, with temperature treated, where relevant, as a rate modulator rather than a separate governing field. In the context of geosynthetic-reinforced systems, FEM has been extended beyond linear elastic approximations to incorporate viscoelastic, elasto-plastic, and anisotropic constitutive laws. The selection of constitutive models remains central to FEM accuracy. For soil behavior, the Mohr–Coulomb and Drucker–Prager models have been widely adopted due to their simplicity in capturing frictional resistance and yield surfaces. However, these models fail to capture degradation effects due to chemical infiltration or prolonged cyclic loading [48, 49]. For geosynthetics, linear elastic or bilinear tensile constitutive laws are often assumed; however, several studies, such as [3, 50], have shown that PET and HDPE exhibit nonlinear stiffness degradation under acidic and saline conditions, necessitating time-evolving material properties. Chemical effects have been incorporated into FEM through two primary mechanisms: (1) direct modification of material parameters (e.g., tensile modulus or interface strength as a function of pH or exposure time), and (2) implementation of degradation laws as user-defined subroutines, optionally scaled by Arrhenius/WLF temperature factors when depth-filtered temperatures are available. In practice, concentration- or time-dependent degradation has been embedded in FEM via user subroutines to update stiffness and interfaces each increment; fully coupled chemo-mechanical implementations have been demonstrated in adjacent materials (e.g., reactive clays and cementitious systems) and directly transferred to geosynthetics [51–54]. However, most models still consider chemical degradation as an external input rather than an endogenous feedback from transport-reaction processes, which is a key limitation in current practices. Although fully coupled transport–reaction–mechanics formulations exist, most studies still implement chemical effects via prescribed parameter-reduction laws (e.g., stiffness and interface updates driven by exposure history) rather than solving the chemistry inside the mechanical step; see Sect. 3.1.1 for the implementation details [34, 45, 55].

3.1.1 Implementation Patterns for Chemo-Mechanical Behaviour (UMAT/USDFLD/UEL)

In practice, chemo-mechanical degradation in geosynthetic-reinforced subgrades is implemented in finite elements by introducing internal state variables that evolve with chemical exposure and cyclic loading, and by updating the constitutive stiffness and interface capacity incrementally at each integration point. Temperature enters as a rate modifier (Arrhenius/WLF shift), consistent with its attenuated role at subgrade depth; no thermal Partial Differential Equation (PDE) is required unless site conditions demand it.

i. **State variables and driving histories**

c: chemical exposure descriptor(s) (e.g., pH proxy, ionic strength, salinity class)

N: cyclic count or equivalent damage time

$D \in [0, 1]$: continuum damage variable for polymer/soil matrix (0 = pristine; 1 = fully degraded)

$b \in [0, 1]$: interface bonding coefficient (scales peak shear/traction)

T: local (depth-filtered) temperature used only in rate multipliers

Table 3 Comparative summary of computational models for coupled problems

Modeling family	Core strengths	Typical limitations	Computational cost	Coupling maturity	Best-fit use	Reference
FEM (elastic–plastic/viscoelastic)	Broad boundary conditions, contact/interaction, scalable meshes; easy to add user subroutines; UMAT/USDFLD	Chemistry is often prescribed (parameter decay) unless co-solved; interface laws are simplified	High–very high (3D, cyclic)	Partial → high (if linked to transport)	Layered subgrades; parametric studies; design	[39–41]
CDM (continuum damage mechanics)	Mesh-objective softening; time-dependent degradation via damage	Needs rich data for calibration; localization without regularization	Moderate–high	Partial (chemistry via damage law)	Progressive stiffness/strength loss; fatigue	[42–44]
Multiphysics (transport–reaction–mechanics)	Solves concentration/temperature fields with kinetics; feedback to stiffness and interface	Integration complexity; adaptive mesh refinement (AMR) needed; expensive	High–very high	High	Spatial gradients, ingress front tracking	[45–47]

Optional: κ(hardening), γ(viscous strain), ϕ(transport saturation index)

ii. **Constitutive form (bulk)**

A degraded elastic/viscoelastic law:

$$\sigma = \mathrm{C}(D) : \varepsilon^e, \mathrm{C}(D) = (1-D)\ \mathrm{C}_0\ (\mathrm{orpiecewiseC}(D, N, c))$$

with optional time–temperature shift for viscoelastic terms: $t_T = t \cdot a_T(T)$ where a_T follows Arrhenius or WLF.

iii. **Interface law (contact/cohesive)**

A peak shear (or traction) is degraded via b:

$$\tau_{\max}(t, c, T) = \tau_0 e^{-\alpha(t,c)\, t} s_T(T),$$
$$\alpha(t, c) = \alpha_0 + \alpha_c(c),$$
$$0 \leqslant b = \tau_{\max}/\tau_0 \leqslant 1$$

with $s_T(T) = \exp[-E_a/R\,(1/T - 1/T_{\mathrm{ref}})]$ or an equivalent WLF factor.

iv. **Evolution laws (example, parsimonious)**

$$\dot{D} = k_D(c)\ s_T(T)\ f(\varepsilon, N), \dot{b} = -k_b(c)\ s_T(T)\ g(\Delta u_t, N)$$

where k_D, k_b are calibrated from soaking + cyclic tests; f, g encode strain/slip-amplitude and cycle-count effects.

v. **Where the subroutines come in**

- USDFLD or Vector User-Defined Field (VUSDFLD): updates field variables $\{D, b, c, N\}$ based on the current exposure step and measured/counted cycles.
- UMAT or Vectorized User Material (VUMAT): computes σ and the consistent tangent $\partial\sigma/\partial\varepsilon$ using the degraded stiffness $\mathrm{C}(D)$ and returns updated state variables.
- UEL (optional for cohesive elements): implements a traction–separation law with $\tau_{\max}(t, c, T)$ and degradation of stiffness/area via b.

vi. **Operator-split coupling (stable and cheap)**

We adopt a staggered loop, transport/exposure → state update → mechanics, which is sufficient when the Jacobian coupling is moderate and consistent with temperature acting as a moderator.

vii. **Consistent tangent and convergence**

Use the degraded tangent $\mathrm{C}(D)$ inside the Gauss-point Jacobian; include simple $\partial\mathrm{C}/\partial D \cdot \partial D/\partial\varepsilon$ terms if strong coupling to strain is modeled. For interfaces, linearize the traction–separation relation around the current b and slip.

viii. **Calibration workflow (minimal, reproducible)**

- Chemistry block: constant-pH soaking at T_{ref}; fit $k_D(c)$(bulk) and $\alpha(c)$(interface) to tensile/pullout/shear strength retention curves.
- Cyclic block: constant-environment cyclic direct shear/pullout; fit $f(\cdot)$ and $g(\cdot)$ vs. slip amplitude and N.
- Temperature factor: adopt literature activation energy (polymer-specific) or WLF constants; validate with a $\pm 10°\mathrm{C}$ sensitivity around T_{ref} (temperature acts as a multiplier).
- Validation: reproduce an independent dataset (different c, Nor layered profile) without re-tuning.

ix. **When a monolithic solve is warranted**

Use a fully coupled reactive-transport mechanics step (and add a heat equation) only when chemistry or heat release is demonstrably stress-dependent or when rapid temperature transients at depth are relevant. For most buried-subgrade cases, thermal effects are attenuated, so the moderator strategy above suffices.

Our UMAT/USDFLD/UEL pattern, grounded in CDM with temperature shift factors and chemistry-sensitive interfaces, follows established Finite Element (FE) damage mechanics and polymer durability practice, and uses operator-splitting from reactive-transport literature [56–59].

3.2 Damage Mechanics Models

To account for progressive material deterioration, CDM introduces scalar or tensorial damage variables into the constitutive relationships, modifying stiffness and strength based on accumulated degradation. In the context of reinforced subgrades, scalar damage formulations have been applied to geosynthetics to simulate chemical embrittlement and fatigue-induced cracking [60, 61]. CDM enables the mesh-independent representation of softening and stiffness reduction; however, its accuracy heavily depends on proper calibration using aging and mechanical tests under coupled loading, with temperature histories used to scale reaction/creep rates. Damage accumulation under cyclic loading and chemical exposure is inherently time-dependent. A deterioration law parameterized by exposure duration, pH, and loading frequency has been proposed to predict the decay of tensile strength in woven PET geotextiles [29]. These formulations often follow Arrhenius-type (or exponential)

decay, with Arrhenius/WLF shift factors applied as temperature multipliers and are embedded within FEM or CDM frameworks. However, the limited availability of long-term laboratory data restricts the calibration of such laws across geosynthetic types.

3.3 Multi-Physics Coupling Strategies

Capturing the full complexity of degradation processes demands multi-physics simulation tools that simultaneously solve chemical transport, reaction kinetics, and mechanical equilibrium, with temperature treated as a rate modulator on reaction and creep. Recent developments by [46, 62] have seen the integration of transport-reaction models (e.g., Fickian diffusion or advection–dispersion) with mechanical solvers. A transport–reaction–mechanical FEM model has been employed to simulate chloride-induced deterioration of HDPE geomembranes [63], where ionic concentration gradients governed stiffness loss and interface friction. Such approaches allow for dynamic updating of material properties based on evolving chemical fields.

We couple transport–reaction to mechanics and, where warranted, scale reaction and creep rates by temperature factors rather than solving a full thermal field. Concretely, the reaction rate uses an Arrhenius modifier $k\left(T\right)=k_0\exp\left[-E_a/\left(RT\right)\right]$, and viscoelastic/creep terms adopt a shift factor $a_T\left(T\right)$ (Arrhenius or WLF). These factors multiply the chemical and damage evolution laws (e.g., $\dot{D}\propto k\left(T\right)$, $\dot{b}\propto k\left(T\right)\ a_T$), while the mechanical equilibrium remains unchanged. This preserves numerical stability and cost, consistent with the temperature's moderating role at subgrade depth. A heat equation with a source term $Q=\left(-\Delta H\right)\ r\left(c,T\right)$ (positive for exothermic, negative for endothermic) is introduced only when laboratory/field evidence indicates significant thermal feedback (e.g., shallow reinforcement, intense reaction zones, or rapid transients); otherwise, a prescribed depth-filtered $T\left(z,t\right)$or constant T_{ref} with sensitivity bounds is sufficient. Since temperature acts as a rate moderator while the mechanical equilibrium remains unchanged, we adopt the following operator-split sequence:

i. **Exposure update**: advance chemistry c^k(from soaking profile or transport solve) and cycles N^k; evaluate temperature factor(s) $k\left(T^k\right)$, $a_T\left(T^k\right)$using a depth-filtered T^k.

ii. **State update (USDFLD)**: update degradation variables (e.g., D^k,b^k) using laws $\dot{D}\propto k\left(T\right)\ f\left(\varepsilon,N,c\right)$, $\dot{b}\propto k\left(T\right)\ a_T\ g\left(\Delta u_t,N,c\right)$.

iii. **Mechanics (UMAT/UEL)**: assemble with degraded stiffness/interface capacity; solve equilibrium; store updated state variables.

Despite their promise, multi-physics models face several technical challenges.

i. **Nonlinearity**

- **Path-Dependent Behavior:** Both chemical degradation and mechanical responses exhibit nonlinear and path-dependent characteristics. This nonlinearity complicates the convergence of numerical methods used in simulations. Traditional linear solvers may struggle to find solutions, resulting in increased computational time and potential inaccuracies in the results [55, 64].
- **Advanced Numerical Techniques:** To address this challenge, researchers are developing advanced numerical techniques, such as adaptive algorithms and robust iterative solvers, that can handle the complexities of nonlinear behavior more effectively. These methods aim to enhance convergence rates and stability in simulations that involve nonlinear interactions [65, 66].

ii. **Time-Dependence**

- **Different Time Scales:** The evolution of viscoplastic behavior, cyclic fatigue, and chemical kinetics occurs over different time scales, making it challenging to capture the interactions between these processes accurately [67–69]. For instance, chemical reactions may occur on a much faster timescale than mechanical deformation, leading to challenges in synchronizing the simulations.
- **Multi-Scale Modeling Approaches:** To address this issue, multi-scale modeling approaches are being employed. These approaches enable the integration of different time scales by utilizing techniques such as homogenization or coupling methods that link fast and slow processes [70–72]. This enables a more comprehensive understanding of how time-dependent behaviors impact overall system performance.

iii. **Interface Tracking**

- **Property Changes at Interfaces:** Soil-geosynthetic interfaces experience property changes due to various factors, including chemical interactions and mechanical loading. These changes necessitate adaptive meshing or cohesive zone modeling to represent the evolving properties of the interface accurately [4, 73, 74].

- **Adaptive Meshing Techniques:** Researchers are exploring adaptive meshing techniques that dynamically adjust the mesh resolution based on the evolving interface characteristics [75]. This enables a more accurate representation of interface behaviour without incurring excessive computational costs. Cohesive zone models are also being developed to simulate failure and interaction at interfaces more effectively [76].

To address these issues, researchers have begun implementing operator-splitting techniques, hybrid solvers, and adaptive time-stepping, with examples spanning geotechnical reactive transport and multiphysics FEM [45, 55], and more general multi-physics frameworks [77, 78]. Although modular coupling and hybrid solvers have been explored, they often assume weak interaction between transport and mechanics or rely on monolithic strategies with high computational cost. Operator-splitting remains essential where chemical transport dynamically alters stiffness, permeability, or boundary conditions; in such cases, a sequential yet strongly coupled solution (transport → mechanics), with temperature as a rate modifier, improves stability and preserves tractability at the field scale [79, 80]. This is particularly relevant when reaction-diffusion modifies interface properties (see Fig. 5), requiring time-consistent updates to mechanical constitutive/damage laws.

To guide model selection and benchmarking in coupled analyses, Table 4 compares FEM, CDM, and fully coupled

Table 4 Comparative summary of modeling frameworks for coupled degradation in geosynthetic-reinforced subgrades

Dimension	FEM	CDM	Multiphysics
Primary objective	Practical chemo-mechanical response via exposure-driven parameter updates	Mesh-objective stiffness/strength softening via internal variables	Solve transport + kinetics + mechanics with state updates
Chemistry handling	External input (pH/time curves) mapped to E, c, ϕ, interface $\tau_{\max}$	Damage variables $D(t,c)$, $b(t,c)$ evolve with exposure	Explicit concentration field $c(x,t)$ drives $D, b, E(c), k(c)$
Interface modeling	Contact or cohesive zone model with $\tau_{\max}(t,c,T)$; slip-weakening optional	Damage-aware cohesive zone model/contact; bond variable $b(t,c)$	Chemistry-sensitive cohesive zone model/contact updated from local $c(x,t)$
Temperature treatment	Arrhenius/WLF multipliers on rates (no heat PDE)	Same; temperature scales $\dot{D}, \dot{b}$ (moderator)	Same by default; add heat equation only if strong exo/endothermic feedback
Physics breadth	Mechanics (+ rate-scaled chemistry)	Mechanics + internal damage kinetics	Transport + kinetics + mechanics (optionally heat)
Calibration data	Soaking curves (strength/modulus) + cyclic tests for interfaces	Soaking + cyclic tests to fit k_D, k_b, $f(\varepsilon, N)$, $g(\Delta u_t, N)$	Soaking + cyclic tests plus basic transport data (D, sorption)
Scalability (1–5)	5 (network studies)	4 (meso–macro)	2–3 (benefits from splitting/uncertainty quantification/surrogates)
Chemical transport fidelity (1–5)	2 (prescribed histories)	3 (implicit via D, b laws)	5 (explicit transport/kinetics)
User extensibility (1–5)	4 (USDFLD/UMAT for updates)	4 (UMAT/UEL damage & cohesive zone model)	3 (heavier implementation/maintenance)
Integration complexity (1–5)	2 (light)	3 (state/tangent management)	5 (PDE coupling, stability, step control)
Strengths	Fast; easy to calibrate; robust for design envelopes	Mesh-objective softening; clear link to tests; good for interfaces	Highest physical fidelity; captures feedback loops
Limitations	No endogenous transport; risk of mis-specifying exposure	Needs rich data; parameter identifiability	Expensive; complex numerics; transport data required
Best-fit use cases	Screening, sensitivity, lifecycle policy, network-level	Interface performance, layered systems, fatigue trends	Sites with known chemical gradients, research-grade studies
Representative patterns	Parameter-reduction + Arrhenius/WLF	CDM + chemistry-sensitive cohesive zone model	Operator-split; monolithic when stress-dependent transport
Typical outputs	Settlement, modulus retention, $\tau_{\max}$ loss vs. time	Damage maps, stiffness/strength decay, interface softening	Concentration, damage/softening fields, coupled settlements

Scales: 1 = low; 5 = high. Temperature is treated as a rate moderator (Arrhenius/WLF) across all frameworks; a heat equation is added only where strong thermal feedback is evidenced

Note: Although multiphysics coupling has high integration complexity (Level 5), field-scale feasibility and numerical stability are commonly achieved using an operator-splitting (staggered) strategy: transport/exposure → state update → mechanics, which avoids monolithic Jacobians while preserving strong sequential coupling

Multiphysics approaches based on the dimensions most relevant to reinforced subgrades.

3.4 Benchmarks and Case Studies

Several benchmark studies have calibrated the cyclic response of reinforced subgrades using FEM, capturing modulus loss and settlement under repeated loads (e.g., laboratory/field-informed studies) [63, 81, 82]. Similarly, a Machine Learning-based Finite Element Method (ML–FEM) surrogate trained on parametric simulations of geosynthetic response to sulfate exposure and dynamic loading achieved > 90% prediction accuracy while substantially reducing computational time [83]. Temperature effects, when relevant at subgrade depth, have been incorporated parsimoniously as Arrhenius/WLF rate multipliers rather than a separate heat equation, maintaining tractability in benchmarking. While benchmark models provide valuable insights, they often suffer from:

i. Over-simplified boundary conditions (e.g., constant chemical concentrations)
ii. Lack of three-dimensional modeling (most remain axisymmetric or 2D plane strain)
iii. Poor scalability to field-scale applications due to computational demands

There is an urgent need for standardized benchmarking frameworks that incorporate both chemical and mechanical loading histories, interface degradation calibration, and validation with large-scale laboratory or field data.

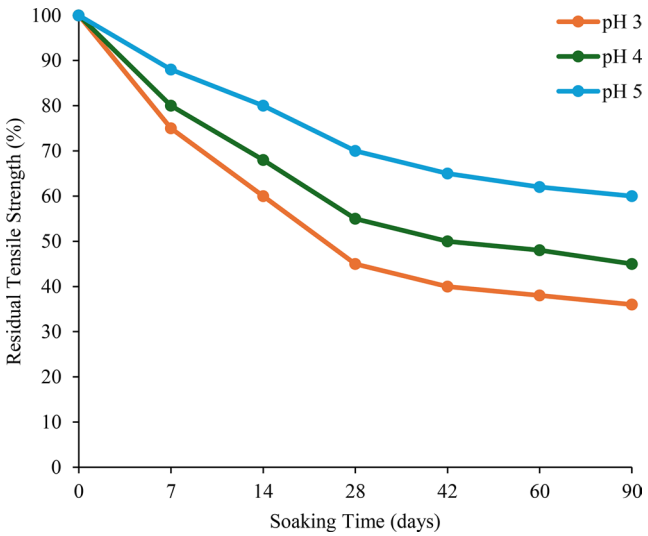

Fig. 6 Synthetic degradation trajectories calibrated to reported trends for PET/PP under acidic soaking; see hydrolysis/aging datasets in [25], polyolefin aging in [7], and interface under chemistry in [4, 6], with preservation of early-time acceleration and late-time plateau

4 Experimental Inputs for Model Calibration and Validation

Numerical predictions of chemo-mechanical degradation in geosynthetic-reinforced subgrades depend on the quality of the experimental datasets used to calibrate them. Laboratory testing provides the essential empirical basis for defining model parameters, validating degradation laws, and refining simulations that aim to capture coupled chemical and mechanical deterioration. This section outlines the key experimental inputs required to support high-fidelity computational models, focusing on chemical soaking protocols, mechanical performance tests, and experimental–computational interfacing.

4.1 Chemical Aging and Soaking Protocols

Chemical degradation, particularly in acidic and saline environments, significantly affects the long-term performance of geosynthetics. Subgrades subjected to acid rain, landfill leachates, or industrial runoff are exposed to pH values ranging between 3 and 5, triggering hydrolysis, polymer chain scission, and bond weakening in polyester-based geosynthetics [84, 85]. Figure 6 presents a comparative degradation profile of geosynthetic strength under acidic soaking conditions at pH levels of 3, 4, and 5 over 90 days. The observed nonlinear trends indicate accelerated strength loss during the initial exposure period (0–28 days), followed by a gradual plateau, suggesting rapid hydrolysis kinetics that stabilize as molecular reorganization reaches saturation. For instance, the tensile strength at pH 3 dropped by over 50% within the first 28 days, whereas at pH 5, it exhibited a slower 25% degradation. Such profiles are critical for parameterizing damage models that incorporate time-dependent weakening. To ensure experimental fidelity, soaking should be conducted in temperature-controlled environments, with chemical replenishment every 7 days to maintain consistent ion concentrations [29, 86]. Measurement of pH drift, visual polymer discoloration, and loss of tensile strength is recommended for degradation benchmarking. These soaking and conditioning protocols define the boundary conditions for the subsequent cyclic and static plate load tests, providing the time-concentration envelope and pH history that will later be used for model calibration (see the workflow in Fig. 7).

4.2 Mechanical Testing Under Cyclic and Static Loading

Mechanical testing quantifies the progressive loss in structural performance following chemical exposure and supports calibration of fatigue, modulus, and settlement

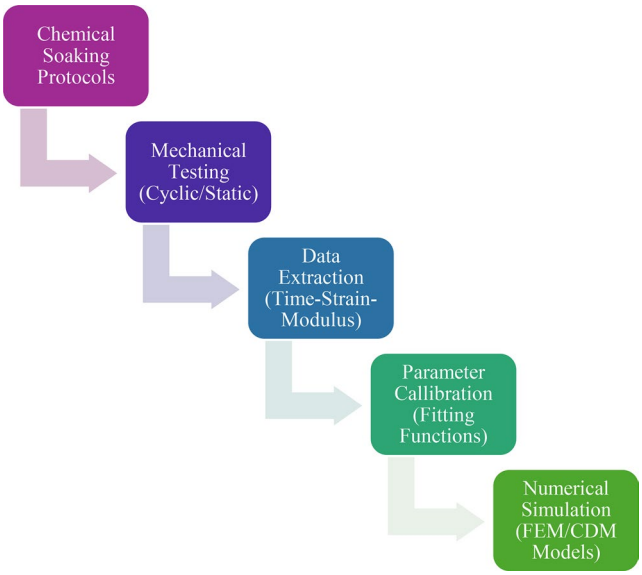

Fig. 7 The experimental–computational coupling diagram

behaviour under simulated service conditions. Table 5 summarizes key mechanical test methods, their control parameters, degradation indicators, and test limitations. Each test type offers distinct insights:

i. **CBR (Soaked & Unsoaked):** While widely used due to simplicity, CBR tests are limited in dynamic fidelity. However, they provide comparative insight into stiffness retention and are often used to benchmark initial deterioration [93, 94].
ii. **Cyclic Triaxial:** Offers control over confining pressures and cyclic amplitudes, simulating multi-directional stress states. The resilient modulus losses of 25–30% were reported for acid-exposed woven PET samples over 1000 cycles [7], capturing both stiffness degradation and strain accumulation.
iii. **Static and Repeated Plate Load Tests:** More field-representative, particularly for layered soil systems. The chemically degraded geotextile-reinforced subgrades demonstrated up to a 42% increase in creep deformation under repeated loads [81].

These tests can be tailored with embedded sensors (strain gauges, pore pressure transducers) to allow real-time data acquisition. Multi-cycle degradation profiles, particularly under varying frequencies (0.1–1 Hz), enable extrapolation to traffic conditions. The measured resilient modulus loss, strain accumulation, and rut depth trajectories yield time–strain–modulus datasets. In Sect. 4.3, we transform these datasets into calibration functions and identify the minimal parameter sets required by FEM/CDM implementations.

4.3 Experimental–Computational Interface

Bridging experimental results with numerical simulations involves multiple data transformations and calibrations. Building on the exposure matrix and mechanical results, we extract peak/residual values and fit exponential or piecewise degradation laws for stiffness, interface shear, and transport coefficients; these functions are then mapped to element-level parameters in FEM and CDM formulations. Figure 7 outlines this workflow, from raw experimental protocols to final model validation. The integration begins with:

i. **Chemical Soaking Protocols:** Define exposure conditions (pH, ion concentration, temperature, time).
ii. **Mechanical Testing:** Generate degradation response data (e.g., stiffness reduction, creep curves).
iii. **Data Extraction:** Quantify degradation laws—e.g., modulus vs. time, bond stress decay.
iv. **Parameter Calibration:** Fit constitutive relationships (e.g., exponential decay, bilinear stiffness models, Arrhenius-type rate laws).
v. **Numerical Implementation:** Translate calibrated parameters into FEM/CDM simulations using commercial codes (e.g., ABAQUS, PLAXIS) or custom solvers.

A significant limitation is the scale discrepancy between lab-sized specimens (usually < 300 mm) and field subgrades (>5 m). Interface effects, such as soil-geotextile debonding, may be underestimated in laboratory pull-out tests. Thus, validation using field-scale plate load data remains crucial. To mitigate overfitting during parameter regression, physical interpretability should guide the model selection process [95]. For polymeric reinforcements, exponential stiffness-loss laws are mechanistically consistent with hydrolysis-controlled degradation [96, 97]. Logistic-type forms

Table 5 A comparative summary of mechanical test methods

Test Method	Parameters Controlled	Degradation Metrics	Limitations	Reference
CBR (Soaked & Unsoaked)	Moisture content, compaction, surcharge	CBR index drop, stiffness ratio	Not dynamic, limited depth insight	[87, 88]
Cyclic Triaxial	Confining pressure, cycle count, frequency	Resilient modulus loss, strain accumulation	Requires advanced setup, slow data	[89, 90]
Static Plate Load	Load increment, plate size, and settlement	Modulus of subgrade reaction, load-settlement	Static only, limited fatigue insight	[91]
Repeated Plate Load	Load amplitude, cycle duration, and creep	Creep rate, stiffness degradation, and rut depth	High effort, sensitive to boundary effects	[92]

have been used for structured soils [98] but should not be adopted for geosynthetics without polymer-specific validation. Accurate simulation of chemo-mechanical degradation demands integrated protocols that connect experimental precision with numerical depth. Chemical aging and cyclic loading must be mirrored with equal granularity in computational models. Standardizing chemical soaking protocols, enhancing sensor resolution in mechanical tests, and refining model calibration workflows are essential to achieving high-confidence predictive tools [99, 100]. Future work should prioritize multi-scale experimental datasets and machine-learning-aided parameter optimization to accelerate simulation fidelity and real-world applicability.

Together, the exposure matrix (Sect. 4.1), mechanical response (Sect. 4.2), and calibration functions (Sect. 4.3) establish an experiment-to-model pipeline: laboratory evidence → fitted deterioration laws → simulation-ready parameters. This pipeline underpins the comparative evaluation of computational frameworks presented in Sect. 5.

5 Advanced Computational Tools and Surrogate Modeling

As the complexity of loading conditions and environmental aggressors intensifies, especially for geosynthetic-reinforced subgrades subjected to cyclic and chemical degradation, traditional deterministic simulations, while foundational, lack the flexibility, speed, and adaptability required for real-time assessment and long-term performance prediction. To address these limitations, recent research has focused on data-driven intelligence, multi-scale physical modeling, and lifecycle management optimization. Together, these computational strategies offer a transformative way to simulate subgrade behavior across various degradation stages and predict when, where, and how failure might initiate under changing in-service conditions. To overcome computational limitations, we combine data-driven surrogates (Sect. 5.1), multi-scale resolution strategies (Sect. 5.2), and lifecycle embedding (Sect. 5.3). Figures 8 (lifecycle trajectories) and 9 (strategy map) consolidate the section's results after the detailed discussion.

5.1 Machine Learning and AI-Driven Surrogates

AI and ML have become crucial tools for enhancing or substituting time-consuming numerical simulations with predictive surrogates. As outlined in Table 6, techniques like Gaussian Process (GP) Regression, Artificial Neural Networks (ANNs), and Support Vector Machines (SVMs) have been successfully applied to predict key mechanical properties, such as fatigue life, rut depth, or stiffness loss, based on multivariate input parameters including cyclic stress levels, pH exposure, temperature, and time-dependent deterioration. To capture nonlinear degradation patterns under combined stressors, we employ GP regression as a nonparametric surrogate; GP models have demonstrated high accuracy for fatigue-life prediction under multiaxial loading with quantified uncertainty [102, 103]. Independent of the surrogate choice, acidity can reduce stiffness and interface capacity, while exposure to saline or chloride modifies interfacial properties, trends consistently reported in experimental and review studies [16, 107]. At the same time, Random Forests show promise in feature selection for stress-permeability

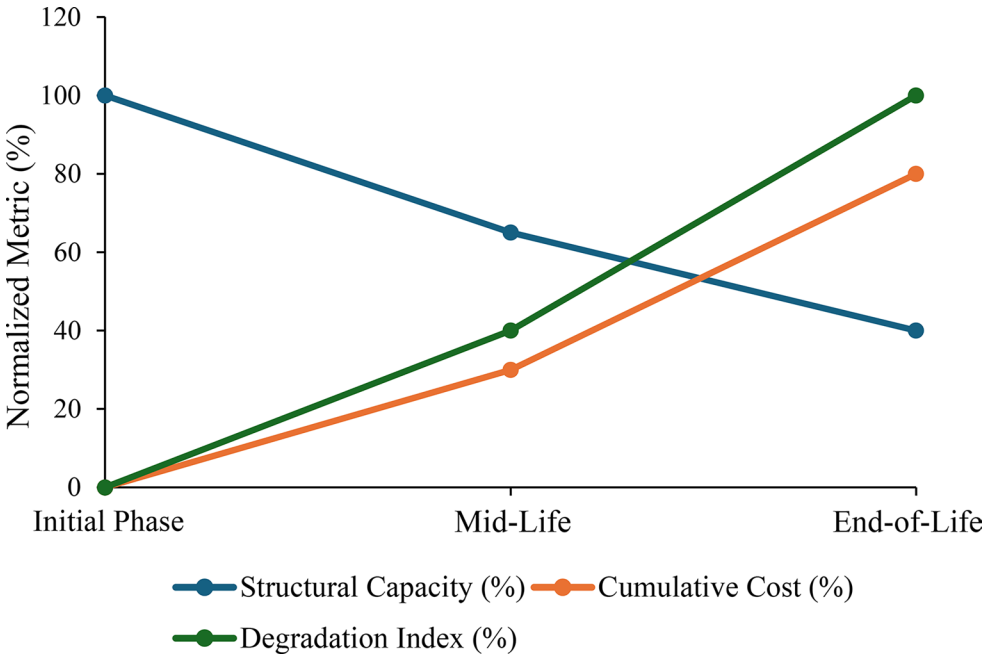

Fig. 8 Lifecycle trends (synthetic example) parameterized to match deterioration/archetype cost growth patterns from stochastic lifecycle studies [101] and field performance syntheses [81]

Table 6 Summary of machine learning techniques for subgrade modelling

Algorithm	Input Features	Target Outputs	Training Data	Performance Metrics	Reference
Gaussian Process	Cyclic load, pH level, fiber type	Stiffness loss, fatigue life	Laboratory tests and field measurements	Prediction error uncertainty bounds	[102, 103]
Artificial Neural Network	Cyclic count, temperature, transport properties	Load capacity, rut depth	In situ monitoring and field measurement	Mean absolute error, R^2	[104]
Random Forest	Modulus, stress, and chloride concentration	Permeability, swelling	Laboratory soaking and mechanical tests	Feature importance Sum of Squared Errors (SSE) error	[105]
Support Vector Machine	Time, geogrid properties, sulfuric attack	Strength retention, creep deformation	Field aging studies	Accuracy root mean squared error	[106]

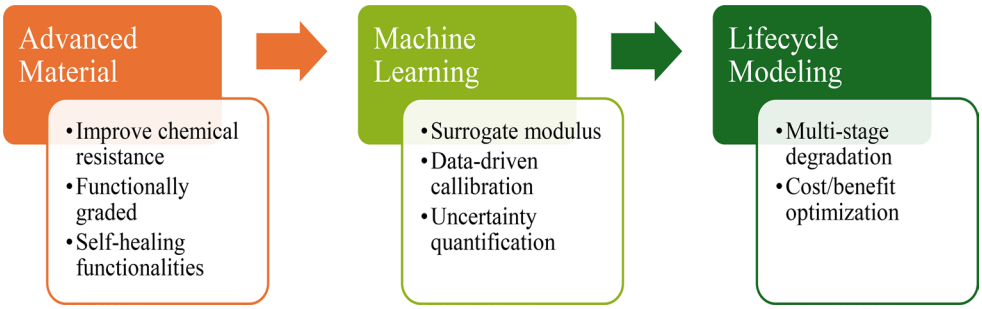

Fig. 9 Strategic future directions for enhancing coupled chemo-mechanical modelling and performance prediction of geosynthetic-reinforced subgrades

response under chloride attack [105]. In Fig. 9, the strategic integration of AI tools is highlighted as a key element in next-generation frameworks. ML is no longer limited to fitting mechanical response curves; it is evolving to perform uncertainty quantification, inverse parameter estimation, and data-driven calibration of constitutive laws. More critically, hybrid architectures such as Physics-Informed Neural Networks (PINNs) are now enabling fusion of physical constraints (e.g., Fickian diffusion, viscoelastic creep, temperature-scaled kinetics) with data streams to maintain model interpretability and extrapolation capability, especially under combined chemical-mechanical loading conditions [108].

5.2 Multi-Scale and Multi-Resolution Simulation Frameworks

Understanding degradation in geosynthetics requires simulation strategies that resolve interactions from molecular chain scission to macroscopic rut formation. This necessitates multi-scale frameworks capable of linking fundamental damage mechanisms at the material level with subgrade-level deformation and failure. Atomistic and meso-scale simulations (e.g., molecular dynamics, lattice spring models) are increasingly employed to simulate chain degradation in geogrids under acid leaching, which then informs damage evolution laws embedded in FEM/CDM models at the macro level [44]. At the domain resolution level, techniques such as adaptive mesh refinement and submodeling help concentrate computational effort in high-gradient zones [109], particularly near geosynthetic-soil interfaces, where degradation initiates and propagates. These localized models are crucial for simulating interfacial cracking, sliding, and detachment, as illustrated conceptually in Fig. 4. The interface-aware resolution strategies strike a balance between simulation efficiency and accuracy, thereby supporting integration into larger infrastructure modeling ecosystems.

5.3 Lifecycle-Based Computational Strategies

Perhaps the most critical advancement lies in embedding lifecycle performance evaluation into degradation-aware modeling frameworks. The long-term evolution of reinforced subgrades, visualized in Fig. 8, captures three co-evolving trajectories:

- **Structural Capacity:** declining from 100% at construction to 40% near the end-of-life due to cumulative degradation,
- **Degradation Index:** escalating linearly or exponentially with exposure to chemical (e.g., acid pH) and mechanical (e.g., cyclic loading) stressors,
- **Cumulative Cost:** increasing nonlinearly as periodic rehabilitation or reinforcement becomes necessary.

These dynamic, coupled trends highlight the limitations of static design methodologies and the need for time-variant computational simulations that integrate structural degradation, exposure conditions, and financial constraints. Modern frameworks now incorporate stochastic deterioration models, probabilistic service life predictions, and multi-objective

optimization to balance safety margins and investment schedules [101]. As indicated in Fig. 9, lifecycle-informed modeling can support cost-benefit analysis, multi-stage degradation planning, and the selection of retrofitting strategies, all of which are essential to sustainable infrastructure asset management. Together, surrogate models, multi-scale simulations, and lifecycle-embedded strategies represent a paradigm shift in subgrade design and performance prediction. By leveraging AI's predictive capabilities, the accuracy of physics-based modeling, and the practicality of lifecycle analytics, computational methods are now capable of providing unprecedented insight, robustness, and efficiency [110, 111], crucial for infrastructure resilience against climate-driven chemical threats and growing mechanical demands. Reliable AI requires (i) high-fidelity labels (joint chemo-mechanical histories and interface metrics), (ii) physics-informed constraints (e.g., mass balance for diffusion, non-negative damage), (iii) uncertainty quantification (GP/PINN) ensembles with prediction intervals), (iv) robust validation (temporal and chemical hold-out sets), and (v) domain-shift tests (generalization to unseen pH–temperature–load regimes) [112–114]. These ingredients elevate ML from curve-fitting to decision-grade surrogates.

6 Critical Gaps and Research Challenges

Despite significant progress in the numerical modelling of geosynthetic-reinforced subgrades under coupled environmental and mechanical actions, several unresolved challenges persist. These limitations compromise the scalability, adaptability, and predictive accuracy of current computational frameworks, especially in chemically aggressive and moisture-sensitive environments. This section identifies and analyzes four significant thematic gaps: the lack of standardized modeling platforms, incomplete chemo-mechanical coupling, the absence of long-term field validation, and inadequate interface modeling under chemical exposure.

6.1 Lack of Standardized Coupled Modeling Frameworks

The geotechnical community currently works within a fragmented simulation landscape. Figure 10 illustrates the interconnected feedback loops resulting from chemical ingress and the redistribution of mechanical stress in geosynthetic-reinforced systems. However, most commercial and

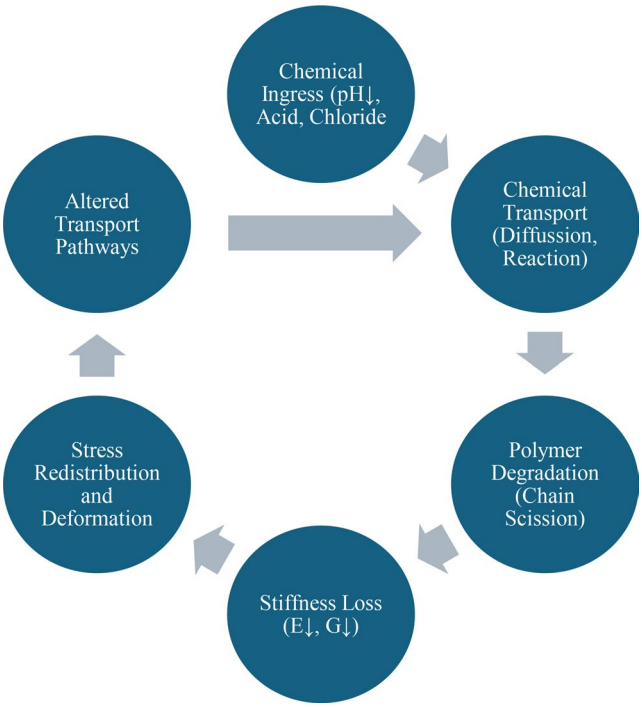

Fig. 10 Coupled chemo-mechanical feedback loops

academic modeling approaches fail to capture this complexity holistically. As summarized in Table 7, FEM platforms, such as PLAXIS, offer excellent scalability and allow for UMAT-based extensibility; however, they lack high-fidelity chemical transport modules [115]. Conversely, Multiphysics platforms (e.g., COMSOL) support native PDE solvers for diffusion-reaction transport but suffer from computational intensity and high integration complexity [47]. CDM frameworks offer moderate capabilities but are limited in terms of extensibility and real-time calibration [42, 43]. There is an urgent need for interoperable frameworks that integrate high-fidelity transport modeling with large-strain mechanics and evolving material laws. Standardization through benchmark datasets and validation scenarios would enable reproducibility and facilitate the deployment of digital twins in subgrade infrastructure systems.

6.2 Incomplete Integration of Chemical Transport with Structural Degradation

The degradation of geosynthetics due to exposure to acid, chloride, and alkaline conditions involves multiple transport and damage mechanisms. Most current models treat these processes separately, simplifying diffusion as a linear

Table 7 Comparative matrix of modeling platforms

Modeling Platform	Scalability	Chemical Transport Fidelity	User Extensibility	Integration Complexity	Reference
FEM (e.g., PLAXIS)	High	Low	High (via UMAT)	Moderate	[115]
CDM	Moderate	Moderate	Moderate	Low	[42, 43]
Multiphysics (e.g., COMSOL)	Low	High	High (built-in PDE modules)	High	[47]

function and decoupling it from mechanical softening [3, 116]. However, Fig. 10 conceptually illustrates how polymer degradation, stiffness loss (elastic stiffness E↓, shear modulus G↓), and altered stress fields actively influence chemical diffusivity, creating a nonlinear feedback loop. Such interactions are not captured in conventional models, which fail to reflect stress-induced permeability evolution or time-dependent reaction kinetics [117]. Advanced formulations are required that incorporate reaction-diffusion equations coupled with modulus degradation laws, as well as adaptive mesh refinement to capture evolving gradients.

6.3 Limited Validation with Long-Term and Field-Scale Data

Another critical barrier is the scarcity of validated field-scale datasets tracking subgrade performance over extended chemical exposure durations. Most simulation-based studies rely on short-term, accelerated aging protocols that may not replicate tropical field conditions [118, 119]. The discrepancy between lab-based tank models and real-life pavements, particularly in terms of interface boundary conditions and moisture variations, limits their transferability to real-world applications [120, 121]. Table 8 compiles major studies and highlights the lack of sensor-instrumented validations and chemical-mechanical coupled data streams. The integration of fiber optic sensors, pH probes, and displacement transducers embedded within geosynthetics could yield transformative insights into long-term degradation, enabling the calibration of inverse models.

6.4 Challenges in Modeling Soil-Geosynthetic Interfaces Under Chemical Influence

Perhaps the most overlooked area is the dynamic loss of interface strength parameters, especially adhesion, interlocking, and shear strength, during chemical attack. Figure 11 presents laboratory-derived synthetic data showing a sharp drop in interface shear strength (%) and bonding coefficient as pH exposure duration increases from 0 to 90 days. Despite this, numerical models typically assume constant contact stiffness or reduction factors not linked to degradation indices. Time-dependent interface laws calibrated from pullout/creep and cyclic shear tests exist, yet chemical coupling in interface elements remains rare in FEM/CDM practice [128–130]. There is a strong research imperative to develop chemically adaptive interface elements that evolve in response to pH, ionic species, and exposure cycles. To operationalize this need, we propose a parsimonious, calibration-ready formulation that embeds chemical exposure directly into the evolving interface strength. A practical chemistry-sensitive interface law is

$$\tau_{max}\,(t, pH) = \tau_0 e^{-\alpha t} 10^{-\beta(pH_{ref} - pH)}$$

where α captures cyclic/time-dependent softening observed in cyclic/direct-shear programs and β scales the well-documented pH-sensitivity of polyester hydrolysis and interface weakening; the form is consistent with exponential damage evolution and the logarithmic definition of pH [4, 131].

We next illustrate calibration and predictive use of this law with a representative laboratory dataset. The PET

Table 8 Studies on geosynthetic-reinforced subgrades under environmental loading

Location/Environment	Soil Type	Geosynthetic Used	Monitoring Techniques	Test Duration	Degradation Metrics	Reference
Texas, USA/Semi-arid and arid regions	Expansive clay	Geogrid	Moisture sensors, condition surveying, and automated plate load testing	Not specified, but long-term performance is evaluated	Tensile strength loss, settlement, and rut depth	[122, 123]
Alberta, Canada/Freeze-thaw	Silty clay	Novel Polymeric Alloy (NPA) Type-D geocell, NPA Type-C geocell, geocomposite	Pressure cells, thermocouples, and moisture sensors	12 months	Load transfer ratio, stress distribution angle, traffic-induced stress, and settlement	[124]
Wuhan, China/Flood conditions	Sandy soil, clayey soil	Geocell, geotextile, composite system	Stress, settlement, acceleration, and pore water pressure monitoring	Not specified	Stress reduction, settlement, acceleration reduction and pore water pressure	[125]
Telangana, India/Tropical-heavy rainfall	Lateritic clay	Biaxial geogrid	CBR tests, pavement thickness design	Not explicitly stated	Bearing capacity ratio (BCR), pavement thickness reduction	[126]
Chandigarh, India/Tropical-heavy rainfall	Sandy soil, clayey soil	Woven geotextile, non-woven geotextile	CBR tests, numerical validation	Not explicitly stated	BCR, numerical model accuracy, and strain localization	[127]

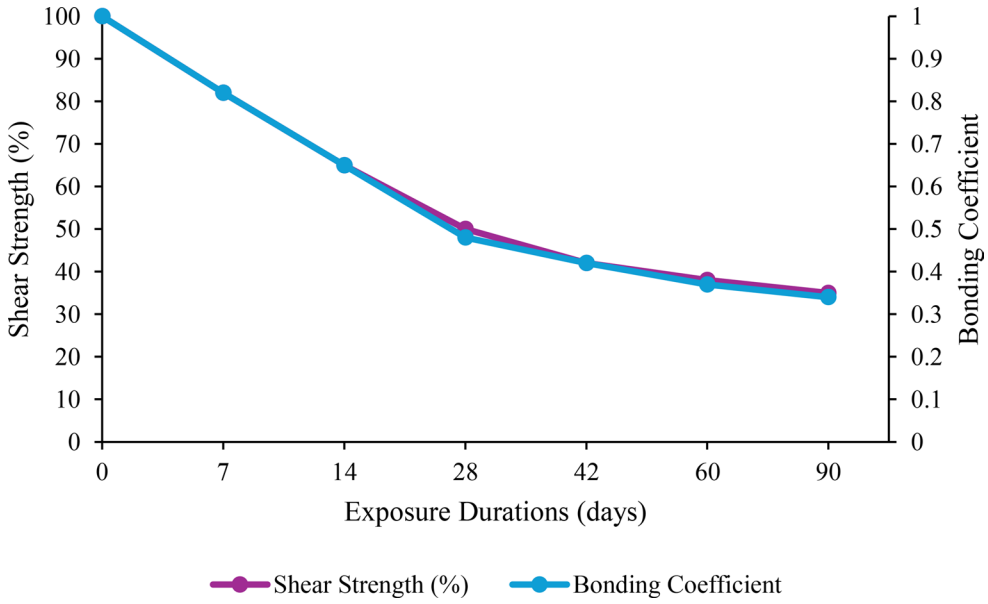

Fig. 11 Synthetic interface-property evolution grounded in chemistry-sensitive interface studies under cyclic shear and leachate exposure [4] and tensile/short-term damage models [117]

geogrid–soil interface under acidic leachate was tested using laboratory cyclic plate loading, combined with 28-day acid soaking, which resulted in an approximately 35% reduction in bond strength and increased deformation [28]. A CDM–FEM model with the interface law above, calibrated to the test's time–pH history, reproduced the measured strength loss and settlement trajectory within experimental scatter, highlighting the importance of coupling transport-reaction with interface damage.

Bridging these modeling gaps requires a comprehensive overhaul of current simulation methods, from algorithmic coupling to field-based parameterization. Future work should focus on developing modular, scalable, and reactive modeling platforms that incorporate chemical-aware constitutive laws and integrate long-term monitoring data to validate deterioration functions. This approach will enable predictive, real-time simulations for durable subgrade design in chemically active environments.

7 Future Research Directions

As geomechanical infrastructure systems face increasing environmental and operational stressors, computational modeling needs to advance beyond single-physics, deterministic tools. This section describes a crucial roadmap across four innovation pillars: open-source solver development, digital twin integration, experimental benchmarking, and sustainability-focused modeling. These advances, supported by advanced tools and frameworks, are shown in Figure 12 and Tables 9–10, collectively moving toward a new paradigm of predictive, adaptive, and environmentally conscious geotechnical modeling.

7.1 Development of Open-Source Coupled Chemo-Mechanical Solvers

The continued reliance on proprietary platforms such as PLAXIS or COMSOL imposes limitations on extensibility, transparency, and financial accessibility, especially in resource-constrained research environments. As shown in Table 9, it is essential to leverage and expand open-source platforms, such as OpenGeoSys, FEniCS, and Kratos Multiphysics, to support reactive transport, mechanical degradation, and chemical–mechanical coupling within a unified system architecture. Each of these platforms allows custom PDE formulation, facilitating the direct modeling of coupled chemo-mechanical systems such as:

i. Reaction–diffusion–deformation loops relevant to acid rain or sulfate attack.
ii. Polymer degradation models within geosynthetics, governed by pH-dependent kinetics.
iii. Adaptive meshing and parallel solvers are necessary for spatially heterogeneous fields.

These features are essential for simulating soil-reinforcement systems where localized degradation (e.g., interfacial scission) must be modeled in tandem with structural response [77, 133]. By integrating open-source tools into academic and practical environments, future research can democratize computational geomechanics, ensuring reproducibility and worldwide accessibility.

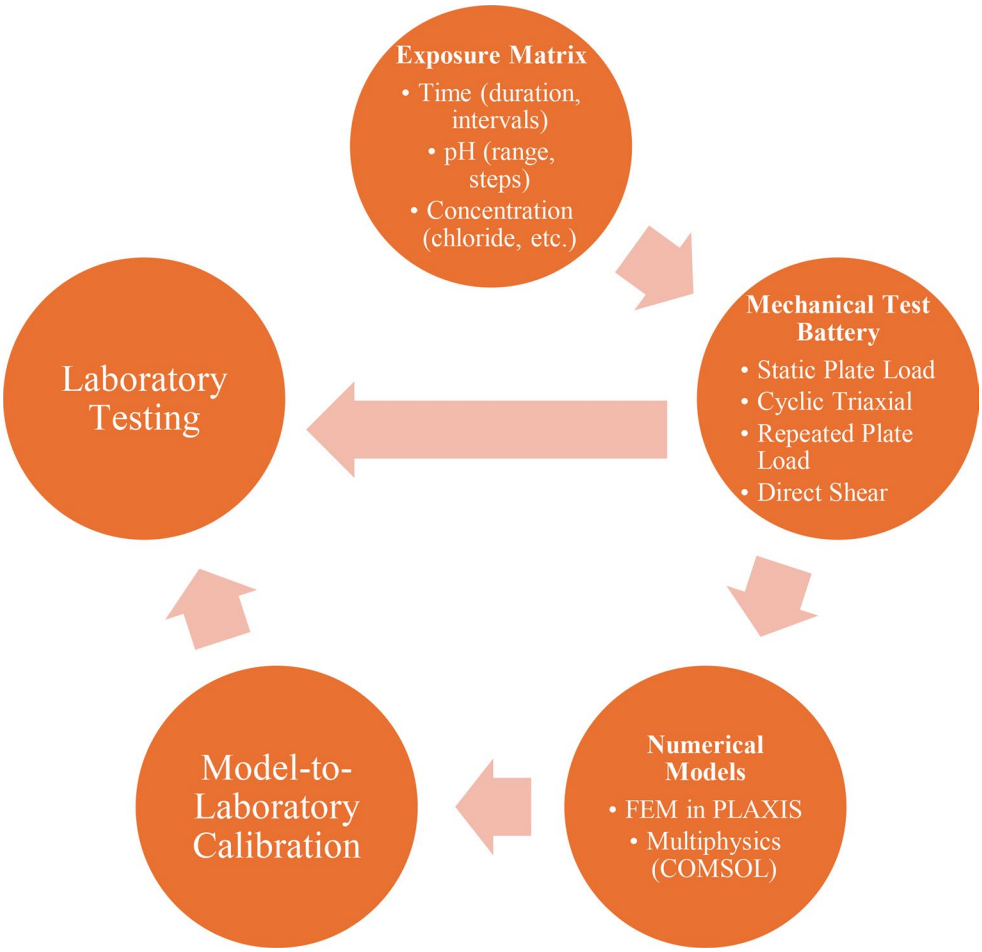

Fig. 12 Schematic benchmarking framework: exposure matrix, mechanical test battery, and model-to-lab calibration routes

Table 9 Comparative capabilities of emerging open-source chemo-mechanical platforms

Platform	Chemical Transport	Mechanical Modeling	Custom PDE Support	Parallelization	Example Application	Reference
OpenGeoSys	✓	✓	✓	✓	Reactive transport in geotechnics	[45]
FEniCS	✓	✓	✓	✓	Deformation–reaction coupling	[132]
Kratos Multiphysics	✓	✓	✓	✓	Soil–structure–chemical interaction	[78]

7.2 Integration of FEM and Field Data: Toward a Digital Twin for Subgrades

The integration of real-time sensor data into numerical frameworks establishes the foundation of digital twins. This transformative concept enables virtual subgrade models to evolve continuously in response to field measurements [134, 135]. Sensor arrays measuring temperature, moisture, pressure, and even pH can be embedded in the subgrade to inform a continuously updated FEM environment. This bi-directional feedback loop offers several advantages:

i. Predictive failure detection well before traditional visual inspections.
ii. Live calibration of stiffness degradation laws based on observed softening.
iii. Reinforcement optimization informed by in-situ chemical exposures and traffic loads.

Such frameworks are especially critical in tropical climates, where chemical ingress rates and hydro-mechanical cycles are highly dynamic on a seasonal basis. Coupling field data with numerical updates enables infrastructure that is not only monitored but also actively self-calibrating.

7.3 Benchmarking Standards for Unified Model Validation

One of the persistent challenges in chemo-mechanical modeling of geosynthetics is the lack of standardized validation protocols. Although American Society for Testing and Materials (ASTM) and International Organization for

Table 10 Integration of sustainability metrics into chemo-mechanical modeling pipelines

Indicator	Measured Through	Coupled With	Computed Output	Reference
Embodied CO_2	Material databases	Geosynthetic thickness	kg CO_2/m^2 reinforced	[136, 137]
Life-cycle cost	Maintenance schedules	Mechanical degradation laws	\$/year of service life	[118, 138]
Environmental risk index	Toxicity profiles	Chemical transport outputs	Risk score	[139]

Standardization (ISO) standards exist for individual mechanical and chemical testing of geosynthetics, they remain fragmented and rarely provide coupled, multi-environment benchmarks and model-to-lab validation workflows. This creates difficulties in validating chemo-mechanical models across laboratories. Laboratories worldwide employ diverse soaking durations, chemical concentrations, and mechanical test setups, resulting in non-transferable calibration datasets. To address this, we propose a benchmarking framework, as illustrated in Fig. 12, which systematically unifies:

i. Exposure matrices defining controlled pH ranges, time intervals, and chemical species (e.g., chloride, sulphate).
ii. A mechanical test battery including static/repeated plate load, cyclic triaxial, and direct shear tests.
iii. Calibration routes between numerical models (PLAXIS, COMSOL) and laboratory degradation data.

This cycle ensures that models are not only fitted to a local context but are also validated against globally replicable datasets. Such protocols thereby raise validation standards in geomechanics to match those in structural and biomedical fields. Our proposal is not to import biomedical standards per se, but to adopt the biomedical discipline's structured benchmarking logic, which includes exposure matrices, test batteries, and model-to-laboratory calibration routes, to ensure reproducible and transferable datasets.

7.4 Embedding Sustainability Indicators in Chemo-Mechanical Pipelines

Modern infrastructure modeling must evolve to quantify not just mechanical performance but also environmental and economic externalities. As outlined in Table 10, computational models should now integrate:

i. Embodied carbon footprints for each reinforcement layer, computed using material databases and coupled to reinforcement volume.
ii. Life-cycle cost analysis, driven by maintenance intervals linked to predicted degradation.
iii. Environmental risk indices, derived from chemical transport simulations and toxicity thresholds.

Such integration is crucial for life-cycle-informed decision-making in road design, particularly in developing regions that strive for carbon neutrality and circular material use. Future models should interact with platforms like openLCA or SimaPro, thereby closing the loop between mechanics, chemistry, and ecological sustainability.

The next generation of geotechnical computational tools must go beyond isolated simulations and develop into multidisciplinary digital frameworks. The integration of open-source platforms, field-sensor feedback, benchmark validation, and environmental metrics transforms modeling into a proactive, intelligent infrastructure solution. These research directions establish the foundation for resilient and predictive design strategies that are technically sound, globally accessible, and environmentally responsible.

8 Conclusions

Chemo-mechanical degradation in geosynthetic-reinforced subgrades arises from the coupled action of chemical transport/reaction and cyclic loading, with temperature acting primarily as a rate modulator (accelerating hydrolysis/oxidation and creep) rather than a dominant driver at subgrade depth. Our review shows that recent models, which are FEM with calibrated parameter reduction, CDM with internal variables, and multiphysics FE with transport–reaction, can each reproduce selected behaviors (modulus loss, interface softening, settlement trends), but predictive fidelity drops when interface chemistry, evolving transport pathways (crack-assisted diffusion), and load history interact over service lifetimes. A pragmatic pattern is emerging to implement chemistry-sensitive state variables (damage D, bond b) and interface laws in UMAT/USDFLD/UEL; update them from exposure histories or a transport step; and, where warranted, scale rates by Arrhenius/WLF factors to reflect depth-filtered temperature. This operator-split workflow (transport → state update → mechanics) offers stability and cost control for field-scale problems, while monolithic solutions remain reserved for cases with strong stress-dependent transport or significant heat release. What remains scarce are standardized, coupled benchmarks that link exposure matrices to cyclic mechanical tests and enforce standard calibration/validation practices. Importantly, the benchmarking framework proposed in Sect. 7.3 and illustrated in

Figure 12 is a tangible, practice-ready deliverable of this review, providing a standardized exposure–testing–calibration workflow that future chemo–mechanical studies can adopt to validate models consistently and transparently across laboratories and codes. To convert these insights into deployable tools for design and asset management, we recommend the following, each with a concrete deliverable.

i. **Standardized benchmarking kits:** Publish an open protocol that pairs (a) exposure matrices (pH/salinity/soaking time, T_{ref} with ±10 °C bounds) with (b) cyclic direct shear/pullout and resilient modulus/creep tests. Deliverables: machine-readable datasets (time–pH–modulus; τ–δ–cycles), uncertainty envelopes, and a minimal reproducible example for model calibration.
ii. **Interface law adoption:** Use an explicit chemistry-sensitive interface law (e.g., $\tau_{\max}(t, \mathrm{pH})$ with time/pH terms) in reinforced-soil checks; calibrate α(time/cycles) from cyclic tests and β(chemistry) from soaking campaigns, where α represents time-/cycle-dependent softening (fatigue/creep-driven bond decay), and β quantifies the pH sensitivity of interface shear strength (chemistry-driven weakening). Report parameter posteriors, not single values.
iii. **Temperature as moderator:** Treat temperature via rate multipliers (Arrhenius/WLF) and seasonal depth filtering; avoid a heat PDE unless exo/endothermic feedback is demonstrated. Always include a $\pm 10°C$ sensitivity on life predictions.
iv. **Validation discipline:** Validate each model against two independent datasets (one chemistry-dominant, one load-dominant) and one layered-profile case to test interface realism; document splits (train/validate) and pre-registered acceptance metrics (e.g., root mean square error, bias, coverage).
v. **Field-scale validation as a mandatory step:** Because laboratory specimens (<300 mm) cannot fully reproduce field boundary conditions, confinement, and interface stress paths in real subgrades (>5 m), at least one field-scale plate load test dataset should be treated as a mandatory validation target for any proposed coupled model to ensure transferability and credibility beyond laboratory calibration.
vi. **Uncertainty & surrogates:** Deploy physics-informed surrogates (GP/PINN with monotonicity or mass-balance constraints) to propagate uncertainty in exposure histories (pH, salinity, moisture, temperature) to maintenance timing; publish calibration code and uncertainty quantification workflows.
vii. **Practice-ready reporting:** Accompany model outputs with actionable Key Performance Indicators (KPIs); residual strength trajectories, interface safety factors vs. exposure time, and lifecycle cost/CO_2 overlays to support intervention scheduling and material selection.

In sum, the field is ready to move from case-specific fits to standardized, auditable pipelines: coupled tests → calibrated interface/bulk laws → operator-split FE with temperature moderation → uncertainty-aware lifecycle decisions. By adopting the steps above, researchers and agencies can turn chemo-mechanical models into credible decision aids for resilient, sustainable subgrade design and management, without over-complicating thermal physics where it is not the primary driver.

Terminology and Implementation Glossary

1. **UMAT:** User-defined material subroutine that updates stress and tangent stiffness from a constitutive law using internal state variables (e.g., damage D). *Common analogs:* custom constitutive model interfaces in general FE codes; user material models in open-source FE.
2. **USDFLD:** User-defined field-variable update subroutine that evolves state descriptors (e.g., D, b, exposure proxy c, cycle count N) as a function of time, cycles, and exposure history. *Common analogs:* field-update callbacks; external state-update scripts coupled to FE.
3. **UEL:** User-defined element subroutine used to implement specialized elements (e.g., cohesive/interface elements with chemistry-sensitive traction–separation and evolving $\tau_{\max}$). *Common analogs:* custom interface/cohesive elements; user element Application Programming Interfaces (APIs) in open-source multiphysics.

Acknowledgements The authors would like to express their sincere gratitude to their respective institutions and research centres for the continuous support provided throughout the development of this review. Special thanks are extended to colleagues and peers who provided constructive feedback and insightful discussions, which significantly enriched the quality of the work. The authors also acknowledge the valuable resources and access to literature provided by institutional libraries, which were instrumental in the comprehensive analysis conducted in this study. This work did not receive any specific grant from funding agencies in the public, commercial, or not-for-profit sectors.

Author Contributions NRM led the conceptualization of the study, designed the research framework, and wrote the initial draft of the manuscript. MA conducted the critical literature review, contributed to the refinement of the methodology, and supported manuscript editing. FA provided academic supervision and technical guidance throughout the development of the paper and reviewed the final manuscript for clarity and accuracy. SNLT contributed to data interpretation, provided constructive feedback on the manuscript, and assisted in enhancing the scientific depth of the discussion.

Funding Open access funding provided by The Ministry of Higher Education Malaysia and Universiti Sains Malaysia. No funding was

received for conducting this study.

Data availability No datasets were generated or analysed during the current study.

Declarations

Competing interests The authors declare no competing interests.

References

1. Badiger M, Mamatha KH, Dinesh SV (2025) Laboratory study on the performance evaluation of RCA reinforced with geosynthetics for GSB layer application in low volume roads. Sustain Mater Technol 44. https://doi.org/10.1016/J.SUSMAT.2025.E01393
2. Calvarano LS, Palamara R, Leonardi G, Moraci N (2016) Unpaved road reinforced with Geosynthetics. Procedia Eng 158:296–301. https://doi.org/10.1016/J.PROENG.2016.08.445
3. Carneiro JR, Almeida F, Carvalho F, de L LM (2023) Tensile and tearing properties of a geocomposite mechanically damaged by repeated loading and abrasion. Materials 16(21). https://doi.org/10.3390/MA16217047
4. Kwak C, Park J, Jang D, Park I (2017) Dynamic shear degradation of geosynthetic-soil interface in waste landfill sites. Appl Sci (Switz) 7(12). https://doi.org/10.3390/APP7121225
5. Chen A, Su C, Chen J, Tang X, Yuan Z (2020) Experimental study on the shear stiffness and damping ratio of the coarse-grained soil against geogrid interface. J Educ Chang Vibroeng 22(7):1606–1617. https://doi.org/10.21595/JVE.2020.21204
6. Kwak CW, Park IJ, Park JB (2014) Chemical and cyclic degradation of geosynthetic-soil interface. Asian J Chem 26(17):5535–5540. https://doi.org/10.14233/AJCHEM.2014.18150
7. Kiersnowska A, Fabianowski W, Koda E (2020) The influence of the accelerated aging conditions on the properties of polyolefin geogrids used for landfill slope reinforcement. Polymers 12(9). https://doi.org/10.3390/POLYM12091874
8. Koerner RM, Hsuan YG, Koerner GR (2017) Lifetime predictions of exposed geotextiles and geomembranes. Geosynth Int 24(2):198–212. https://doi.org/10.1680/JGEIN.16.00026
9. Naga L, Chikhaoui M, Cazzuffi D, Djerbal L (2025) Effect of installation damage on the behavior of a polypropylene geogrid in an aggressive environment. Transp Geotech 51. https://doi.org/10.1016/J.TRGEO.2025.101523
10. Zaabar I, Chatti K (2014) Estimating vehicle operating costs caused by pavement surface conditions. Transp Res Rec 2455:63–76. https://doi.org/10.3141/2455-08
11. Ram P, Peshkin D (2014) Performance and benefits of Michigan department of Transportation's capital preventive maintenance program. Transp Res Rec 2431(1):24–32. https://doi.org/10.3141/2431-04
12. Tsai Y, Wu Y, Lewis Z (2013) Full-lane coverage micromilling pavement-surface quality control using emerging 3D line laser imaging Technology. J Transp Eng 140(2). https://doi.org/10.1061/(ASCE)TE.1943-5436.0000604
13. Gajo A, Cecinato F, Hueckel T (2016) Chemo-mechanical coupling in bonded geomaterials: representations in two scales. Geotechnical Spec Publ 137–146. https://doi.org/10.1061/9780784480120.015
14. Lu X, Yang Y, Cai Q, Zhou W, Ao Z, Yang Z (2024) Effect of different types of additives on the interface transition zone of geopolymer rock interface. Caikuang Yu Anquan Gongcheng Xuebao/J Min Saf Eng 41(4):790–800. https://doi.org/10.13545/J.CNKI.JMSE.2023.0392
15. Guimarães MGA, de C UD, Urashima BMC (2023) Durability of geotextiles exposed to accumulated weathering and liquid factors. Int Rev Psychiatr Civ Eng 14(6):479–488. https://doi.org/10.15866/IRECE.V14I6.23585
16. Gao J, Yang Y, Bian X, Zhu G (2024) Study on dynamic shear properties of sulfate saline soil-geotextile interface with different salt content. Soil Dyn Earthquake Eng 183. https://doi.org/10.1016/J.SOILDYN.2024.108807
17. Jabbour M, Metalssi OO, Quiertant M, Baroghel-Bouny V (2022) A critical review of existing test-Methods for external sulfate attack. Materials 15(21). https://doi.org/10.3390/MA15217554
18. Carneiro JR, Almeida PJ, Lopes MDL (2018) Laboratory Evaluation of interactions in the degradation of a polypropylene geotextile in marine environments. Adv Mater Sci Eng 2018. https://doi.org/10.1155/2018/9182658
19. Carneiro JR, Morais M, Lopes M de L (2018) Degradation of polypropylene geotextiles with different chemical stabilisations in marine environments. Construct Building Mater 165:877–886. https://doi.org/10.1016/J.CONBUILDMAT.2018.01.067
20. Derombise G, Van Schoors LV, Bourmaud A, Davies P (2012) Morphological and physical evolutions of aramid fibers aged in a moderately alkaline environment. J Appl Polym Sci 123(5):3098–3105. https://doi.org/10.1002/APP.34923
21. Anjana RK, Keerthana S, Arnepalli DN (2023) Coupled effect of UV ageing and temperature on the diffusive transport of aqueous, vapour, and gaseous phase organic contaminants through HDPE geomembrane. Geotext Geomembr 51(2):316–329. https://doi.org/10.1016/J.GEOTEXMEM.2022.11.005
22. Chen SX, Xu Y, Qiang LY, Xin NC, Dong L, Cai LJ, Fei HQ (2019) Evolution of geomembrane degradation and defects in a landfill: impacts on long-term leachate leakage and groundwater quality. J Cleaner Prod 224:335–345. https://doi.org/10.1016/J.JCLEPRO.2019.03.200
23. Ferrazzo ST, de S TR, Bragagnolo L, Prestes E, Korf EP, Prietto PDM, Ulsen C (2020) Effects of acidic attack on chemical, mineralogical, and morphological properties of geomaterials. Environ Sci Pollut Res 27(30):37718–37732. https://doi.org/10.1007/S11356-020-09834-6
24. Guo J, Zhou Y, Guo H, Min W (2021) Saline and alkaline stresses alter soil properties and composition and structure of gene-based nitrifier and denitrifier communities in a calcareous desert soil. BMC Microbiol 21(1). https://doi.org/10.1186/S12866-021-02313-Z
25. Dubelley F, Planes E, Bas C, Pons E, Yrieix B, Flandin L (2018) Predictive durability of polyethylene terephthalate toward hydrolysis over large temperature and relative humidity ranges. Polymer 142:285–292. https://doi.org/10.1016/J.POLYMER.2018.03.043
26. Müller WW, Jakob I, Tatzky-Gerth R, Wöhlecke A (2016) A study on antioxidant depletion and degradation in polyolefin-based

geosynthetics: sacrificial versus regenerative stabilization. Polym Eng Sci 56(2):129–142. https://doi.org/10.1002/PEN.24199
27. Maduna L, Patnaik A, Nayak R (2022) The use of the box-Behnken experimental design to model tensile strength of spun-laced fabrics and evaluating fabrics behaviour in acidic condition. J Ind Textiles 51(6):837–855. https://doi.org/10.1177/1528083719894640
28. Alibeiki Y, Hassanlourad M, Ghasemipanah A (2022) Effect of acidic and alkaline pore fluid on the mechanical properties of fine-grained soil. Bull Eng Geol Environ 81(12). https://doi.org/10.1007/S10064-022-02998-0
29. Silva RA, Abdelaal FB, Rowe RK (2025) A 9-year study of the degradation of a HDPE geomembrane liner used in different high pH mining applications. Geotext Geomembr 53(1):230–246. https://doi.org/10.1016/J.GEOTEXMEM.2024.09.012
30. Guimarães MGA, de OP, de C UD, Pereira EL, Urashima BMC (2023) Cyclic fatigue durability of woven geotextiles for use in sustainable waste-dewatering systems. Sustainability (Switz) 15(18). https://doi.org/10.3390/SU151813807
31. Chowdhury T, Wang Q, Enyoh CE (2022) Degradation of polyethylene terephthalate microplastics by mineral acids: experimental, molecular modelling and optimization studies. J Polym The Environ 30(12):5211–5227. https://doi.org/10.1007/S10924-022-02578-Z
32. Celina MC (2013) Review of polymer oxidation and its relationship with materials performance and lifetime prediction. Polym Degrad Stabil 98(12):2419–2429. https://doi.org/10.1016/J.POLYMDEGRADSTAB.2013.06.024
33. Arhant M, Le Gall M, Le Gac PY, Davies P (2019) Impact of hydrolytic degradation on mechanical properties of PET - Towards an understanding of microplastics formation. Polym Degrad Stabil 161:175–182. https://doi.org/10.1016/J.POLYMDEGRADSTAB.2019.01.021
34. Le Traon C, Aquino T, Bouchez C, Maher K, Le Borgne T (2021) Effective kinetics driven by dynamic concentration gradients under coupled transport and reaction. Geochim Cosmochim Acta 306:189–209. https://doi.org/10.1016/J.GCA.2021.04.033
35. Robert DJ, Rajeev P (2016) A modified Mohr-Coulomb model to simulate the response of buried pipes subjected to large ground displacement. Geotechnical Spec Publ 410–421. https://doi.org/10.1061/9780784480120.042
36. Jie YM, Wang J, Yu LF, Ting LJ, Qi CS (2022) Analysis of cyclic shear characteristics of reinforced soil interfaces under cyclic loading and unloading. Geotext Geomembr 50(1):99–115. https://doi.org/10.1016/J.GEOTEXMEM.2021.09.004
37. Abras J, Hosseinverdi S, Jude D, Sitaraman J, Hariharan N (2025) Machine learning based surrogate model Development using GPU driven computational simulations. AIAA Sci Technol Forum Exposition AIAA SciTech Forum 2025. https://doi.org/10.2514/6.2025-0040
38. Kopiika N, Karavias A, Krassakis P, Ye Z, Ninic J, Shakhovska N, Argyroudis S, Mitoulis SA (2025) Rapid post-disaster infrastructure damage characterisation using remote sensing and deep learning technologies: a tiered approach. Automation in Construction 170. https://doi.org/10.1016/J.AUTCON.2024.105955
39. Carvalho PRP, Coda HB, Sanches RAK (2023) A large strain thermodynamically-based viscoelastic-viscoplastic model with application to finite element analysis of polytetrafluoroethylene (PTFE). Eur J Criminol Mech - A/Solids 97. https://doi.org/10.1016/j.euromechsol.2022.104850
40. Takaoka H, Sakaue K (2020) Evaluation of viscoelastic-viscoplastic characteristics and finite element analyses for thermoplastics. Adv Compos Mater 29(3):273–284. https://doi.org/10.1080/09243046.2019.1699268
41. Thapa S, Cheng YT (2025) Flat punch indentation in viscoelastic materials: analytical, experimental, and finite element analysis results. Mech Time Depend Mater 29(1). https://doi.org/10.1007/s11043-024-09747-8
42. Menzel A, Sprave L (2020) Continuum damage mechanics-modelling and simulation. Solid Mech Its Appl 262:231–256. https://doi.org/10.1007/978-3-030-31547-4_8
43. Subramanyam N, Vijayakumar R, Rao KP (2022) Continuum damage mechanics model for damage assessment and strength prediction in laminated composite structures. J Fail Anal Prev 22(2):633–647. https://doi.org/10.1007/S11668-022-01346-4
44. Zhang K, Badreddine H, Hfaiedh N, Saanouni K, Liu J (2021) Enhanced CDM model accounting of stress triaxiality and lode angle for ductile damage prediction in metal forming. Int J Damage Mech 30(2):260–282. https://doi.org/10.1177/1056789520958045
45. Schweizer D, Prommer H, Blum P, Siade AJ, Butscher C (2018) Reactive transport modeling of swelling processes in clay-sulfate rocks. Water Resour Res Res 54(9):6543–6565. https://doi.org/10.1029/2018WR023579
46. Vasile NS, Doherty R, Monteverde Videla AHA, Specchia S (2016) 3D multi-physics modeling of a gas diffusion electrode for oxygen reduction reaction for electrochemical energy conversion in PEM fuel cells. Appl Energy 175:435–450. https://doi.org/10.1016/J.APENERGY.2016.04.030
47. Wu Y, He Y, Zhang J, Tian W, Su G, Qiu S (2024) Finite element based multi-dimension and multi-physics coupling analysis for nuclear reactor System. Yuanzineng Kexue Jishu/At Energy Sci Technol 58(2):257–271. https://doi.org/10.7538/YZK.2024.YOUXIAN.0032
48. Hadzalic E, Ibrahimbegovic A, Dolarevic S (2018) Failure mechanisms in coupled soil-foundation systems. Coupled Syst Mech 7(1):27–42. https://doi.org/10.12989/CSM.2018.7.1.027
49. Xiaochen W, Jin C, Xiangjun L, Lixi L, Tong L, Xuancheng W, Hongwei L (2023) Statistical damage constitutive model considering water-weakening effect based on the hoek-brown criterion. Environ Earth Sci 82(17). https://doi.org/10.1007/S12665-023-11093-W
50. Amjadi M, Fatemi A (2020) Tensile behavior of high-density polyethylene including the effects of processing technique, thickness, temperature, and strain rate. Polymers 12(9). https://doi.org/10.3390/POLYM12091857
51. Belhadjamor M, Ben BM, Mezlini S, Abed-Meraim F (2024) Development and implementation of a new computational strategy for the prediction of elastoplastic buckling. Int J Appl Mech 16(9). https://doi.org/10.1142/S1758825124500911
52. Liu C, Kelly RG (2019) A review of the application of finite element method (FEM) to localized corrosion modeling. Corrosion 75(11):1285–1299. https://doi.org/10.5006/3282
53. Stepanova L (2019) Computational simulation of damage accumulation processes in cracked bodies by the UMAT procedure of SIMULIA Abaqus. J Phys Conf Ser 1368(4). https://doi.org/10.1088/1742-6596/1368/4/042065
54. Yang ZJ, Yao F, Huang YJ (2020) Development of ABAQUS UEL/VUEL subroutines for scaled boundary finite element method for general static and dynamic stress analyses. Eng Anal Boundary Elem 114:58–73. https://doi.org/10.1016/j.enganabound.2020.02.004
55. Zuo ZC, Bennett T (2021) Modelling of the fully coupled chemo-mechanical degradation for cement-based materials. Proc Inst Civ Eng Eng Comput Mech 174(3):158–175. https://doi.org/10.1680/JENCM.20.00033
56. Álvarez-Vázquez A, Fernández-Canteli A, Ron EC, Fernández PF, Muñiz-Calvente M, Rey MJL (2020) A Novel approach to describe the time-temperature conversion among relaxation curves of viscoelastic materials. Materials 13(8):1809. https://doi.org/10.3390/MA13081809

57. Krauklis AE, Akulichev AG, Gagani AI, Echtermeyer AT (2019) Time-temperature-plasticization superposition principle: predicting creep of a plasticized epoxy. Polymers 11(11):1848. https://doi.org/10.3390/POLYM11111848
58. Lu R, Nagel T, Poonoosamy J, Naumov D, Fischer T, Montoya V, Kolditz O, Shao H (2022) A new operator-splitting finite element scheme for reactive transport modeling in saturated porous media. Comput Geosci 163:105–106. https://doi.org/10.1016/J.CAGEO.2022.105106
59. Wu X, Vanapalli SK (2022) Three-dimensional modeling of the mechanical behavior of a single pile in unsaturated expansive soils during infiltration. Comput Geotech 145:104696. https://doi.org/10.1016/J.COMPGEO.2022.104696
60. Abdul Hamid ZM, Findeisen C, Laveuve DM, Rohrmüller, Richter H, De Monte M, Spancken D, Hohe J (2024) A continuum damage mechanics model for fatigue degradation and failure of short fiber reinforced composites. Compos Sci Technol 254. https://doi.org/10.1016/J.COMPSCITECH.2024.110679
61. Del Solar GG, Martín, Maldonado N (2018) Formulation, implementation and validation of a scalar damage model for brittle materials applied to three-dimensional solid elements. Revista Ing de Constr 33(1):111–122. https://doi.org/10.4067/S0718-50732018000100111
62. Marino A, Peltomäki M, Lim J, Aerts A (2020) A multi-physics computational tool based on CFD and GEM chemical equilibrium solver for modeling coolant chemistry in nuclear reactors. Prog Nucl Energy 120. https://doi.org/10.1016/J.PNUCENE.2019.103190
63. Jain A, Mittal S, Shukla SK (2023) Use of polyethylene terephthalate fibres for mitigating the liquefaction-induced failures. Geotext Geomembr 51(1):245–258. https://doi.org/10.1016/J.GEOTEXMEM.2022.11.002
64. Besson J, Lebon F, Lorentz E (2024) Numerical methods for strong nonlinearities in mechanics: contact and fracture. Numer Methods Strong Nonlinearities Mech: Contact Fract 1–384. https://doi.org/10.1002/9781394340507
65. Guo Y, Cao X, Leng H, Song J (2025) Learning complex nonlinear physical systems using wavelet neural operators. Chin Phys B 34(3). https://doi.org/10.1088/1674-1056/ADA7DC
66. Inderjeet BR (2025) A new iterative Newton Raphson technique for the numerical simulation of nonlinear equations. J Integr Sci Technol 13(4). https://doi.org/10.62110/SCIENCEIN.JIST.2025.V13.1080
67. Benaarbia A, Chatzigeorgiou G, Kiefer B, Meraghni F (2019) A fully coupled thermo-viscoelastic-viscoplastic-damage framework to study the cyclic variability of the Taylor-Quinney coefficient for semi-crystalline polymers. Int J Mech Sci 163. https://doi.org/10.1016/J.IJMECSCI.2019.105128
68. Chen X, Zhao X, Cui X (2025) Isothermal low-cycle fatigue and fatigue-creep of Alloy 709 using an unified viscoplasticity modelling. J Retailing Strain Anal Eng Des. https://doi.org/10.1177/03093247241311956
69. Kindrachuk VM, Unger JF (2017) A fourier transformation-based temporal integration scheme for viscoplastic solids subjected to fatigue deterioration. Int J Fatigue 100:215–228. https://doi.org/10.1016/J.IJFATIGUE.2017.03.015
70. Marques M, Belinha J, Oliveira AF, Manzanares Céspedes MC, Jorge RMN (2020) Application of an enhanced homogenization technique to the structural multiscale analysis of a femur bone. Comput Methods Biomech Biomed Eng 23(12):868–878. https://doi.org/10.1080/10255842.2020.1768377
71. Seo M, Min S (2022) Novel material representation method via a deep learning model for multi-scale topology optimization. Adv Eng Softw 174. https://doi.org/10.1016/J.ADVENGSOFT.2022.103300
72. Wang FY, Xu YL, Qu WL (2014) Mixed-dimensional finite element coupling for structural multi-scale simulation. Finite Elem Anal Des 92:12–25. https://doi.org/10.1016/J.FINEL.2014.07.009
73. Pham TA, Nadimi S, Sutman M (2024) Critical review of physical-mechanical principles in geostructure-soil interface mechanics. Geotechnical Geological Eng 42(8):6757–6808. https://doi.org/10.1007/S10706-024-02954-7
74. Stavropoulou E, Briffaut M, Dufour F, Camps G, Boulon M (2017) A new apparatus for testing the delayed mechanical behaviour of interfaces: the shearing interfaces creep box (SInC box). Comptes Rendus - Mec 345(6):417–424. https://doi.org/10.1016/J.CRME.2017.05.002
75. Beisiegel N, Castro CE, Behrens J (2021) Metrics for performance quantification of adaptive mesh refinement. J Sci Comput 87(1). https://doi.org/10.1007/S10915-021-01423-0
76. Ebadi-Rajoli J, Akhavan-Safar A, Hosseini-Toudeshky H, da Silva LFM (2020) Progressive damage modeling of composite materials subjected to mixed mode cyclic loading using cohesive zone model. Mech Mater 143. https://doi.org/10.1016/J.MECHMAT.2020.103322
77. Li X, Liu X, Chai X, He H, Zhang B, Zhang T (2023) Multi-physics coupling simulation of small mobile nuclear reactor with finite element-based models. Comput Phys Commun 293. https://doi.org/10.1016/J.CPC.2023.108900
78. Yildirim A, Jacobson KE, Anibal JL, Stanford BK, Gray JS, Mader CA, Martins JRRA, Kennedy GJ (2025) Mphys: a modular multiphysics library for coupled simulation and adjoint derivative computation. Struct Multidiscip Optim 68(1). https://doi.org/10.1007/S00158-024-03900-0
79. Nuca R, Storvik E, Radu FA, Icardi M (2024) Splitting schemes for coupled differential equations: Block Schur-based approaches & Partial jacobi approximation[formula presented]. Comput Math Appl 161:190–201. https://doi.org/10.1016/j.camwa.2024.02.042
80. Wong ZY, Kwok F, Horne RN, Tchelepi HA (2019) Sequential-implicit Newton method for multiphysics simulation. J Comput Phys 391:155–178. https://doi.org/10.1016/j.jcp.2019.04.023
81. Hegde AM, Palsule PS (2020) Performance of geosynthetics reinforced subgrade subjected to repeated vehicle loads: experimental and numerical studies. Front Built Environ 6. https://doi.org/10.3389/fbuil.2020.00015
82. Qian J, Zhang JF, Wang Y, Ma X (2015) An equivalent finite element method for traffic-load-induced settlement of pavement on the soft clay subgrade. In Computer Methods and Recent Advances in Geomechanics - Proceedings of the 14th Int. Conference of International Association for Computer Methods and Recent Advances in Geomechanics IACMAG, pp 2014: 1835–1840). https://doi.org/10.1201/b17435-325
83. Meethal RE, Kodakkal A, Khalil M, Ghantasala A, Obst B, Bletzinger KU, Wüchner R (2023) Finite element method-enhanced neural network for forward and inverse problems. Adv Modeling Simul Eng Sci 10(1). https://doi.org/10.1186/S40323-023-00243-1
84. Özçoban MŞ, Acarer S, Tüfekci N (2022) Effect of solid waste landfill leachate contaminants on hydraulic conductivity of landfill liners. Water Sciamp; Technol 85(5):1581–1599. https://doi.org/10.2166/WST.2022.033
85. Raei A, Shayannejad M (2024) Simulation of leachate movement from clay geosynthetic liners using a laboratory model. Agric Res. https://doi.org/10.1007/S40003-024-00819-2
86. Ra ES, Kerry Rowe R, Abdelaal FB (2025) A 10-year study of HDPE geomembrane longevity in contact with low pH solutions. Can Geotechnical J 62. https://doi.org/10.1139/CGJ-2024-0504

87. Henzinger C, Vogt S (2020) Evaluation of the dynamic CBR test on coarse-grained materials. Geotechnical Test J 43(2). https://doi.org/10.1520/GTJ20180269
88. Pasand SA, Nasrollahi N, Asghari-Kaljahi E, Majidian S (2022) Effect of fine material content on the CBR of Iran saturated soils. Innovative Infrastruct Sol 7(6). https://doi.org/10.1007/S41062-022-00964-Z
89. Liu T, Jardine RJ, Vinck K, Ackerley SK (2022) Optimization of advanced laboratory monotonic and cyclic triaxial testing on fine sands. Geotechnical Test J 45(6). https://doi.org/10.1520/GTJ20210190
90. Showkat R, Singh SK, Babu GLS (2025) Evaluation of dynamic properties of unsaturated soils under cyclic loading. Soil Dyn Earthquake Eng 190. https://doi.org/10.1016/J.SOILDYN.2024.109196
91. Kraszewski C, Rafalski L, Ćwiąkała M, Dreger M (2020) Effect of applied stress increments of the secondary deformation modulus and the ratio between the secondary and primary moduli of sandy gravel and crushed aggregate in static plate load tests. Roads Bridges - Drogi i Mosty 19(4):283–296. https://doi.org/10.7409/RABDIM.020.018
92. Shaban AM, Almuhanna RR, Jawad AA (2021) Performance characterization of unsaturated granular soils using static and dynamic plate load test. Geotechnical Test J 44(6):1821–1838. https://doi.org/10.1520/GTJ20200191
93. Muthu Lakshmi S, Geetha S, Selvakumar M (2021) Predicting soaked CBR of SC subgrade from dry density for light and heavy compaction. In Materials Today: Proceedings, vol 45. pp 1664–1670). https://doi.org/10.1016/J.MATPR.2020.08.558
94. Reang RB, Pal SK (2020) Time-dependent CBR values of the Silty-clay soil mixed with fly ash as well as Sand. Lect Notes Civ Eng 85:623–638. https://doi.org/10.1007/978-981-15-6086-6_51
95. Khan S, Sasmal SK, Kumar GS, Behera RN (2021) Assessment of liquefaction potential based on SPT data by using Machine learning approach. Lect Notes Civ Eng 116 LNCE 145–156. https://doi.org/10.1007/978-981-15-9976-7_14
96. Bathurst RJ, Naftchali FM (2021) Geosynthetic reinforcement stiffness for analytical and numerical modelling of reinforced soil structures. Geotext Geomembr 49(4):921–940. https://doi.org/10.1016/j.geotexmem.2021.01.003
97. Bathurst RJ, Naftchali FM, Jamshidi Chenari R (2023) The role of geosynthetic stiffness in soil reinforcement applications. In E3S Web of Conferences, vol 368. https://doi.org/10.1051/e3sconf/202336801002
98. Rodrigues C, Cruz N, Amoroso S, Cruz M (2019) Stiffness decay in structured soils by seismic dilatometer. Geotechnical Test J 43(4). https://doi.org/10.1520/GTJ20180352
99. Alam M, Parol V, Das A (2022) A DEM study on microstructural behaviour of soluble granular materials subjected to chemo-mechanical loading. Geomech Energy Environ 32. https://doi.org/10.1016/J.GETE.2022.100390
100. Catania G, Amadori S (2025) Dynamical calibration of a standard sensor-based experimental test apparatus for accurate material model parametric identification. Sensors 25(7). https://doi.org/10.3390/S25071982
101. Iannacone L, Gardoni P (2024) Modeling deterioration and predicting remaining useful life using stochastic differential equations. Reliab. Eng. Syst. Saf 251. https://doi.org/10.1016/J.RESS.2024.110251
102. Karolczuk A, Skibicki D, Pejkowski Ł (2022) Gaussian process for Machine learning-based fatigue life prediction model under multiaxial stress-strain conditions. Materials 15(21). https://doi.org/10.3390/MA15217797
103. Karolczuk A, Słoński M (2022) Application of the Gaussian process for fatigue life prediction under multiaxial loading. Mech Syst Signal Process 167. https://doi.org/10.1016/J.YMSSP.2021.108599
104. Maraqa F, Al Adwan J, Alzubi Y, Yasin B, Khatatbeh A (2023) Estimating ultimate moment capacity of spirally reinforced concrete columns using various Artificial neural networks. Int Rev Psychiatr Civ Eng 14(4):300–307. https://doi.org/10.15866/IRECE.V14I4.22143
105. Pham BT, Nguyen MD, Al-Ansari N, Tran QA, Ho LS, Van LH, Prakash I (2021) A Comparative study of soft Computing models for prediction of permeability coefficient of soil. Math Probl Eng 2021. https://doi.org/10.1155/2021/7631493
106. Chao Z, Wang H, Hu H, Ding T, Zhang Y (2023) Predicting the temperature-dependent long-term creep mechanical response of silica Sand-textured geomembrane interfaces based on physical tests and Machine learning techniques. Materials 16(18). https://doi.org/10.3390/MA16186144
107. Kwak CW, Park IJ, Park JB (2016) Development of modified interface apparatus and prototype cyclic simple shear test considering chemical and thermal effects. Geotechnical Test J 39(1):20–34. https://doi.org/10.1520/GTJ20140223
108. Jeong I, Cho M, Chung H, Kim DN (2024) Data-driven non-parametric identification of material behavior based on physics-informed neural network with full-field data. Computer Methods in applied mechanics and Engineering 418. https://doi.org/10.1016/J.CMA.2023.116569
109. Stock A, Moureau V (2024) Feature-based adaptive mesh refinement for multi-regime reactive flows. In Proceedings of the Combustion Institute, vol 40. pp 1–4). https://doi.org/10.1016/J.PROCI.2024.105488
110. Karthikeyan C (2024) AI for climate modelling and prediction with Special Reference to empowering India: AI-Driven insights for climate resilience and prediction. Nexus AI, Climatol, Urbanism Smart Cities 91–119. https://doi.org/10.4018/979-8-3693-5918-1.CH004
111. Singh M, Arora V, Kulshreshta K (2024) AI and the environment: innovative approaches to climate change. Maintaining Sustain World The Nexus Environ Sci AI 1–22. https://doi.org/10.4018/979-8-3693-6336-2.CH001
112. Amrihesari M, Banerjee M, Olmedo R, Brettmann B (2025) Role of high fidelity vs. Low fidelity experimental data in Machine learning model performance for Predicting polymer solubility. Macromol Rapid Commun. https://doi.org/10.1002/marc.202500454
113. Hoffmann L, Fortmeier I, Elster C (2021) Uncertainty quantification by ensemble learning for computational optical form measurements. Mach Learn: Sci Technol 2(3). https://doi.org/10.1088/2632-2153/ac0495
114. Maria Tronci E, Downey ARJ, Mehrjoo A, Chowdhury P, Coble D (2025) Physics-informed Machine learning part I: different strategies to incorporate physics into Engineering problems. In Conference Proceedings of the Society for Experimental Mechanics Series, pp 1–6). https://doi.org/10.1007/978-3-031-68142-4_1
115. Schellenberg AH, Huang Y, Mahin SA (2019) Structural finite element software coupling using adapter elements. CMES - Comput Modeling Eng Sci 120(3):719–737. https://doi.org/10.32604/CMES.2019.04835
116. Carneiro JR, Escórcio F, de Lurdes Lopes M (2019) Resistance of geotextiles against the isolated and combined effect of mechanical damage under repeated loading and abrasion. Environ Sci Eng 700–707. https://doi.org/10.1007/978-981-13-2224-2_87
117. Lombardi G, Paula AM, Pinho-Lopes M (2022) Constitutive models and statistical analysis of the short-term tensile response of geosynthetics after damage. Construct Building Mater 317. https://doi.org/10.1016/J.CONBUILDMAT.2021.125972
118. Fladvad M, Erlingsson S (2022) Permanent deformation modelling of large-size unbound pavement materials tested in a heavy

vehicle simulator under different moisture conditions. Road Mater Pavement Des 23(5):1157–1180. https://doi.org/10.1080/14680629.2021.1883464
119. Zhang J, Zhu X, Wang W, Chu H (2023) Experimental simulation for moisture damage of saturated asphalt mixture and evolution of mixture's pore water pressure, accumulative strain. Construct Building Mater 369. https://doi.org/10.1016/J.CONBUILDMAT.2022.130274
120. Chun S, Kim K, Greene J, Choubane B (2015) Evaluation of interlayer bonding condition on structural response characteristics of asphalt pavement using finite element analysis and full-scale field tests. Construct Building Mater 96:307–318. https://doi.org/10.1016/J.CONBUILDMAT.2015.08.031
121. Mousavi S, Ghayoomi M, Dave EV (2021) A system dynamics framework for mechanistic analysis of flexible pavement systems under moisture variations. Transp Geotech 30. https://doi.org/10.1016/J.TRGEO.2021.100619
122. Tamrakar P, Wayne MH (2021) Performance of geogrid stabilized roadways constructed over expansive clay subgrade. Geotechnical Spec Publ 278–287. https://doi.org/10.1061/9780784483695.027
123. Zornberg JG, Roodi GH (2021) Use of geosynthetics to mitigate problems associated with expansive clay subgrades. Geosynth Int 28(3):279–302. https://doi.org/10.1680/JGEIN.20.00043
124. Huang M, Liu J, Pokharel SK, Dagenais T, Chatterjee A, Lin C (2025) Full-scale testing and monitoring of geosynthetics-stabilized flexible pavement in Alberta, Canada. Geotext Geomembr 53(1):427–444. https://doi.org/10.1016/J.GEOTEXMEM.2024.11.003
125. Li L, Sun K, Xu M, Xiao H, Jiang S (2025) Study on the dynamic performance of heavy-load railway reinforced subgrade under flood condition. Geotext Geomembr 53(4):985–998. https://doi.org/10.1016/J.GEOTEXMEM.2025.03.005
126. Vennamaneni S, Aketi NR, Paisa S (2018) Reduction in pavement thickness by using geogrid. Int J Eng Technol (UAE) 7(3):17–20. https://doi.org/10.14419/IJET.V7I3.3.14473
127. Negi MS, Singh SK (2021) Experimental and numerical studies on geotextile reinforced subgrade soil. Int J Multiling Geotechnical Eng 15(9):1106–1117. https://doi.org/10.1080/19386362.2019.1684654
128. Leonardi G, Lo BD, Palamara R, Suraci F (2020) Finite element analysis of geogrid-stabilized unpaved roads. Sustainability (Switz) 12(5). https://doi.org/10.3390/su12051929
129. Wilson L, Morrison M (2025) Erratum for "A critical Evaluation of some constitutive models for finite-element simulation of structural Steel components. J Eng Mech 151(9). https://doi.org/10.1061/JENMDT.EMENG-8535
130. Yin Z, Ndiema KM, Lekalpure RL, Kiptum CK (2022) Numerical study of geotextile-reinforced flexible pavement overlying low-strength subgrade. Appl Sci (Switz) 12(20). https://doi.org/10.3390/app122010325
131. Moraci N, Cardile G, Gioffrè D, Mandaglio MC, Calvarano LS, Carbone L (2014) Soil geosynthetic interaction: design parameters from experimental and theoretical analysis. Transp Infrastruct Geotech 1(2):165–227. https://doi.org/10.1007/S40515-014-0007-2/FIGURES/57
132. Jovanović AP, Loffhagen D, Becker MM (2023) Introduction and verification of FEDM, an open-source FEniCS-based discharge modelling code. Plasma Sources Sci Technol 32(4). https://doi.org/10.1088/1361-6595/ACC54B
133. Müller S, Zech A, Heße F (2021) ogs5py: a python-API for the OpenGeoSys 5 Scientific modeling package. Groundwater 59(1):117–122. https://doi.org/10.1111/GWAT.13017
134. Kalyanaraman S, Ponnusamy S, Harish RK (2024) Amplifying digital twins through the integration of wireless sensor networks: In-depth exploration. Digit Twin Technol AI Implementations Future-Focused Businesses 70–82. https://doi.org/10.4018/979-8-3693-1818-8.CH006
135. Tyagi AK, Richa Tiwari S, Kumari S (2025) Digital twin technology for smart wireless sensor networks. Human-centric integration of next-generation data Science and blockchain Technology. Advancing Soc 5.0 Paradigms: 385-406. https://doi.org/10.1016/B978-0-443-33498-6.00009-1
136. Jalaei F, Masoudi R, Guest G (2022) A framework for specifying low-carbon construction materials in government procurement: a case study for concrete in a new building investment. J Cleaner Prod 345. https://doi.org/10.1016/J.JCLEPRO.2022.131056
137. Parece S, Resende R, Rato V (2024) A BIM-based tool for embodied carbon assessment using a construction classification System. Developments in the Built environment 19. https://doi.org/10.1016/J.DIBE.2024.100467
138. Samuelsson I, Spross J, Larsson S (2023) Integrating life-cycle environmental impact and costs into geotechnical design. Proc Inst Civ Eng Eng Sustainability 177(1):19–30. https://doi.org/10.1680/JENSU.23.00012
139. Sur IM, Micle V, Hegyi A, Lăzărescu AV (2022) Extraction of metals from polluted soils by bioleaching in relation to environmental risk assessment. Materials 15(11). https://doi.org/10.3390/MA15113973
140. de Melo Dl, Kendall A, Jt D (2024) Evaluation of life cycle assessment (LCA) use in geotechnical engineering. Environ Res: Infrastruct Sustainability 4(1). https://doi.org/10.1088/2634-4505/AD2154